Chapter 2
Skew-Ray Tracing of Geometrical Optics

In geometrical optics (or ray optics), light propagation is described in terms of "rays", where each ray is regarded as an idealized narrow bundle of light with zero width [1]. This is different from beam, which is a concept used in almost all fields of physics. Geometrical optics provides equations for predicting the paths followed by the rays through an optical system. These equations are somewhat simplistic, and cannot therefore accurately describe such effects as diffraction and polarization. However, they nevertheless provide a powerful tool for investigating the performance of optical systems during the initial design and analysis stage. Geometrical optics in this book are applied to perform sequential raytracing based on Snell's law and a homogeneous coordinate notation, and then compute the first- and second-order derivative matrices of various optical quantities. Notably, the equations of geometrical optics expressed in terms of homogeneous coordinate notation are often far simpler than their vector counterparts; particularly for more complex optical elements such as prisms.

2.1 Source Ray

In geometrical optics, rays are usually, but not necessarily, assumed to move from left to right. In accordance with the homogeneous coordinate notation used in this book, the incidence point ${}^{g}\bar{P}_{i}$ and unit directional vector ${}^{g}\bar{\ell}_{i}$ at the ith boundary surface are designated as ${}^{g}\bar{P}_{i} = [\,P_{ix} \quad P_{iy} \quad P_{iz} \quad 1\,]^{T}$ and ${}^{g}\bar{\ell}_{i} = [\,\ell_{ix} \quad \ell_{iy} \quad \ell_{iz} \quad 0\,]^{T}$, respectively, where the pre-superscript "g" of the leading symbols ${}^{g}\bar{P}_{i}$ and ${}^{g}\bar{\ell}_{i}$

P.D. Lin, *Advanced Geometrical Optics*, Progress in Optical Science and Photonics 4, DOI 10.1007/978-981-10-2299-9_2

indicates that the components of the respective vectors are referred with respect to coordinate frame $(xyz)_g$. The ray at the ith boundary surface can thus be denoted as

$$^{g}\bar{R}_i = \left[{}^{g}\bar{P}_i \quad {}^{g}\bar{\ell}_i\right]^T = [P_{ix} \quad P_{iy} \quad P_{iz} \quad \ell_{ix} \quad \ell_{iy} \quad \ell_{iz}]^T. \tag{2.1}$$

Note that when ${}^{0}\bar{R}_i$ (or ${}^{0}\bar{P}_i$ or ${}^{0}\bar{\ell}_i$) is referred to the world coordinate frame $(xyz)_0$, the pre-superscript "0" is omitted for reasons of simplicity.

An optical lens or prism (referred to simply as an optical element hereafter) is a block of optical material possessing multiple boundary surfaces and having a constant refractive index. To trace the path of a ray through an optical system with k elements and n boundary surfaces, it is first necessary to label the individual elements within the system from j = 0 to j = k and the boundary surfaces from i = 0 to i = n. By convention, labels j = 0 and i = 0 are assigned to the source ray $\bar{R}_0$, which originates at point source

$$\bar{P}_0 = \begin{bmatrix} P_{0x} \\ P_{0y} \\ P_{0z} \\ 1 \end{bmatrix} \tag{2.2}$$

and travels along the unit directional vector

$$\bar{\ell}_0 = \begin{bmatrix} \ell_{0x} \\ \ell_{0y} \\ \ell_{0z} \\ 0 \end{bmatrix} = \begin{bmatrix} C\beta_0 C(90^\circ + \alpha_0) \\ C\beta_0 S(90^\circ + \alpha_0) \\ S\beta_0 \\ 0 \end{bmatrix}, \tag{2.3}$$

where β_0 is the angle between $\bar{\ell}_0$ and the projection of $\bar{\ell}_0$ on the horizontal plane passing through the origin of a notional unit sphere centered at $\bar{P}_0$ (see Fig. 2.1). Furthermore, α_0 is the angle between the meridional plane and $\bar{\ell}_0$, and is measured along the zenith direction (i.e., the z_0 axis direction) of the unit sphere. For convenience, the cone shown in Fig. 2.1 is referred to hereafter as the $\alpha_0(\beta_0)$ cone, and is generated by sweeping $\bar{\ell}_0$ with a constant value of β_0 around the zenith direction of the unit sphere. It is noted that $\bar{\ell}_0$ is parallel with the y_0 axis when $\alpha_0 = 0^\circ$ and $\beta_0 = 0^\circ$. From Eqs. (2.2) and (2.3), the variable vector $\bar{X}_0$ of the source ray $\bar{R}_0$ is obtained as

$$\bar{X}_0 = [P_{0x} \quad P_{0y} \quad P_{0z} \quad \alpha_0 \quad \beta_0]^T. \tag{2.4}$$

When a point source $\bar{P}_0$ of an axis-symmetrical system is confined to the y_0z_0 plane (where y_0 points along the optical axis of the system), then a meridional ray (or tangential ray) is the ray lying on that plane. Furthermore, the y_0z_0 plane is referred to as the meridional plane. It is noted that in an axis-symmetrical system,

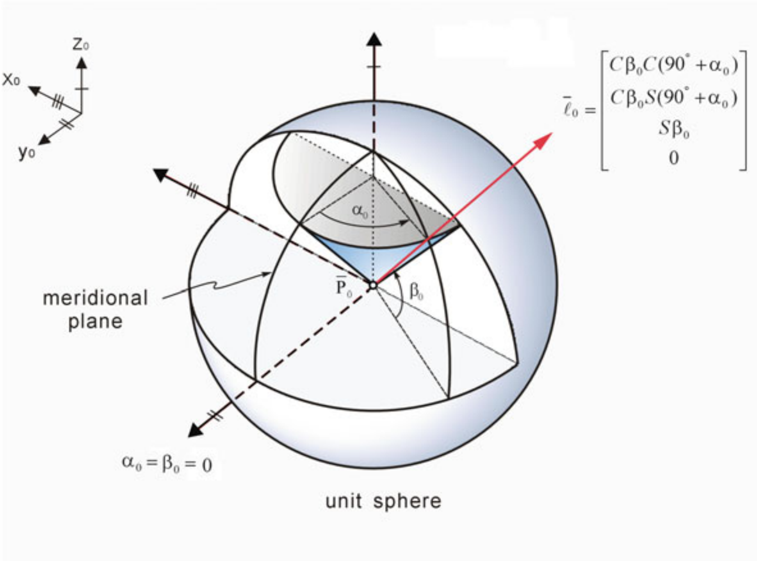

Fig. 2.1 Schematic representation of unit directional vector $\bar{\ell}_0$ originating from point source $\bar{P}_0$

any source ray originating from point source $\bar{P}_0 = [0 \quad P_{0y} \quad P_{0z} \quad 1]^T$ with $\alpha_0 = 0$ always travels on the meridional plane.

The discussions above consider a single ray originating at a single point located at an arbitrary location. Such a point source provides a good approximation for finite but small sources. However, in many practical cases, an expression for the path of perfectly collimated light within the optical system is required. This can most conveniently be achieved by placing a number of source points, each emitting a single ray with a fixed unit directional vector $\bar{\ell}_0$, at several discrete locations in the optical system (Fig. 2.2).

Fig. 2.2 Collimated light comprising multiple parallel light rays

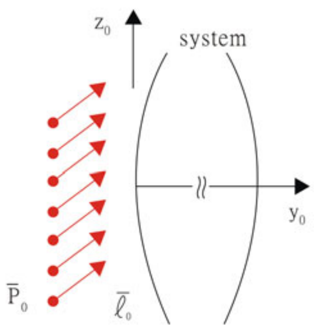

2.2 Spherical Boundary Surfaces

Raytracing is a commonly used technique in geometrical optics for the design, analysis and synthesis of optical systems. The basic foundations of raytracing were presented originally by Hamilton [2] in 1830 and were then further developed by Silverstein [3] in 1918. Raytracing forms the basis of many optical models and techniques [2–33]; with outstanding basic documents written by Spencer et al. [4] and Stavroudis [5] with vector analysis, but most of them use paraxial, meridional or skew ray-tracing with approximations. Accordingly, this chapter presents an analytical skew-ray tracing methodology which is more easily understandable and applied.

2.2.1 Spherical Boundary Surface and Associated Unit Normal Vector

Spherical lenses are one of the most common elements in optical systems. In such lenses, the two boundary surfaces are formed by the partial surfaces of two notional spheres, while the lens axis is ideally perpendicular to both boundary surfaces. The boundary surfaces may be convex (i.e., the sphere center and incoming ray are located on opposite sides of the vertex), concave (i.e., the sphere center and incoming ray are located on the same side of the vertex), or planar (i.e., flat). The line joining the centers of the two spheres making up the lens surfaces represents the axis of the lens. As shown in Fig. 2.3, the generating curve ${}^{i}\bar{q}_{i}$ of a spherical boundary surface, denoted as the ith boundary surface in an optical system, is a curve in the x_iz_i plane with the form

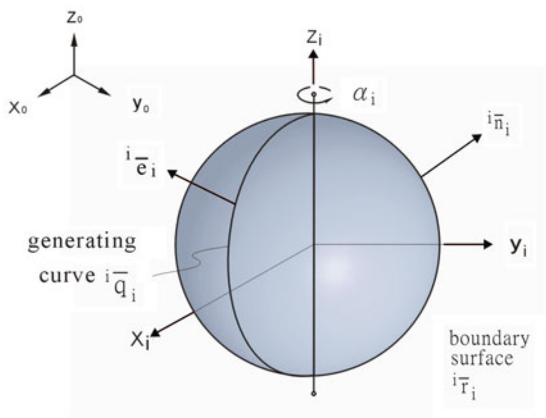

Fig. 2.3 Generating curve and associated unit normal vector of spherical boundary surface

$$
{}^{i}\bar{q}_{i}=\begin{bmatrix} x_i \\ 0 \\ z_i \\ 1 \end{bmatrix}=\begin{bmatrix} |R_i|C\beta_i \\ 0 \\ |R_i|S\beta_i \\ 1 \end{bmatrix}, \frac{-\pi}{2}\le\beta_i\le\frac{\pi}{2}, \tag{2.5}
$$

where $|R_i|$ denotes the absolute value of the radius R_i, and R_i can be either positive or negative, depending on whether the surface is convex or concave, respectively. For any generating curve, there exist two possible unit normal vectors, which point in opposite directions from one another. These unit normal vectors can be formulated as

$$
{}^{i}\bar{\eta}_{i}=\begin{bmatrix} \eta_{ix} \\ \eta_{iy} \\ \eta_{iz} \\ 0 \end{bmatrix}=\frac{s_i}{\sqrt{(dx_i/d\beta_i)^2+(dz_i/d\beta_i)^2}}\begin{bmatrix} dz_i/d\beta_i \\ 0 \\ -dx_i/d\beta_i \\ 0 \end{bmatrix}=s_i\begin{bmatrix} C\beta_i \\ 0 \\ S\beta_i \\ 0 \end{bmatrix}, \tag{2.6}
$$

where s_i is set to either +1 or −1 to indicate the two possible directions of the vector. Having formulated the two unit normal vectors of the generating curve, the spherical boundary surface ${}^{i}\bar{r}_{i}$ and associated unit normal vectors ${}^{i}\bar{n}_{i}$ can be obtained by rotating ${}^{i}\bar{q}_{i}$ and ${}^{i}\bar{\eta}_{i}$, respectively, about the z_i axis through an angle α_i $(0\le\alpha_i<2\pi)$, i.e.,

$$
\begin{aligned}
{}^{i}\bar{r}_{i}=\begin{bmatrix} x_i \\ y_i \\ z_i \\ 1 \end{bmatrix} &= \mathrm{rot}(\bar{z},\alpha_i)\,{}^{i}\bar{q}_{i}=\begin{bmatrix} C\alpha_i & -S\alpha_i & 0 & 0 \\ S\alpha_i & C\alpha_i & 0 & 0 \\ 0 & 0 & 1 & 0 \\ 0 & 0 & 0 & 1 \end{bmatrix}\begin{bmatrix} |R_i|\,C\beta_i \\ 0 \\ |R_i|\,S\beta_i \\ 1 \end{bmatrix} \\
&= \begin{bmatrix} |R_i|\,C\beta_i C\alpha_i \\ |R_i|\,C\beta_i S\alpha_i \\ |R_i|\,S\beta_i \\ 1 \end{bmatrix},
\end{aligned} \tag{2.7}
$$

$$
{}^{i}\bar{n}_{i}=\mathrm{rot}(\bar{z},\alpha_i)\,{}^{i}\bar{\eta}_{i}=s_i\begin{bmatrix} C\alpha_i & -S\alpha_i & 0 & 0 \\ S\alpha_i & C\alpha_i & 0 & 0 \\ 0 & 0 & 1 & 0 \\ 0 & 0 & 0 & 1 \end{bmatrix}\begin{bmatrix} C\beta_i \\ 0 \\ S\beta_i \\ 0 \end{bmatrix}=s_i\begin{bmatrix} C\beta_i C\alpha_i \\ C\beta_i S\alpha_i \\ S\beta_i \\ 0 \end{bmatrix}. \tag{2.8}
$$

Equations (2.7) and (2.8) describe a spherical boundary surface ${}^{i}\bar{r}_{i}$ and its unit normal vector ${}^{i}\bar{n}_{i}$ in terms of two parameters, α_i and β_i. Both equations are expressed with respect to an arbitrary coordinate frame $(xyz)_i$. However, many derivations in this book are built relative to the world coordinate frame $(xyz)_i$. The following pose matrix of $(xyz)_i$ with respect to $(xyz)_0$ is thus required:

$$
\begin{aligned}
{}^0\bar{A}_i &= \mathrm{tran}(t_{ix},0,0)\mathrm{tran}(0,t_{iy},0)\mathrm{tran}(0,0,t_{iz})\mathrm{rot}(\bar{z},\omega_{iz})\mathrm{rot}(\bar{y},\omega_{iy})\mathrm{rot}(\bar{x},\omega_{ix}) \\
&= \begin{bmatrix} C\omega_{iz}C\omega_{iy} & C\omega_{iz}S\omega_{iy}S\omega_{ix} - S\omega_{iz}C\omega_{ix} & C\omega_{iz}S\omega_{iy}C\omega_{ix} + S\omega_{iz}S\ \omega_{ix} & t_{ix} \\ S\omega_{iz}C\omega_{iy} & S\omega_{iz}S\omega_{iy}S\omega_{ix} + C\omega_{iz}C\omega_{ix} & S\omega_{iz}S\omega_{iy}C\omega_{ix} - C\omega_{iz}S\omega_{ix} & t_{iy} \\ -S\omega_{iy} & C\omega_{iy}S\omega_{ix} & C\omega_{iy}C\omega_{ix} & t_{iz} \\ 0 & 0 & 0 & 1 \end{bmatrix} \\
&= \begin{bmatrix} I_{ix} & J_{ix} & K_{ix} & t_{ix} \\ I_{iy} & J_{iy} & K_{iy} & t_{iy} \\ I_{iz} & J_{iz} & K_{iz} & t_{iz} \\ 0 & 0 & 0 & 1 \end{bmatrix},
\end{aligned}
\tag{2.9}
$$

where $t_{ix},\ t_{iy},\ t_{iz}, \omega_{ix}, \omega_{iy}$ and ω_{iz} are the pose variables of the spherical boundary surface. The unit normal vectors $\bar{n}_i$ of the boundary surface with respect to frame $(xyz)_o$ can then be obtained via the following transformation:

$$
\bar{n}_i = \begin{bmatrix} n_{ix} \\ n_{iy} \\ n_{iz} \\ 0 \end{bmatrix} = {}^0\bar{A}_i{}^i\bar{n}_i = s_i \begin{bmatrix} I_{ix}C\beta_i C\alpha_i + J_{ix}C\beta_i S\alpha_i + K_{ix}S\beta_i \\ I_{iy}C\beta_i C\alpha_i + J_{iy}C\beta_i S\alpha_i + K_{iy}S\beta_i \\ I_{iz}C\beta_i C\alpha_i + J_{iz}C\beta_i S\alpha_i + K_{iz}S\beta_i \\ 0 \end{bmatrix}. \tag{2.10}
$$

2.2.2 *Incidence Point*

In Fig. 2.4, a ray originating from incidence point $\bar{P}_{i-1}$ located on the previous boundary surface $\bar{r}_{i-1}$ is directed along the unit directional vector $\bar{\ell}_{i-1}$ and is reflected or refracted at boundary surface $\bar{r}_i$. Any intermediate point $\bar{P}'_{i-1}$ along this ray is given by $\bar{P}'_{i-1} = \bar{P}_{i-1} + \lambda\bar{\ell}_{i-1}$. The parameter $\lambda = \lambda_i$, for which the incoming ray $\bar{R}_{i-1}$ hits the current boundary surface $\bar{r}_i$ at incidence point

$$
\bar{P}_i = \begin{bmatrix} P_{ix} \\ P_{iy} \\ P_{iz} \\ 1 \end{bmatrix} = \begin{bmatrix} P_{i-1x} + \lambda_i\,\ell_{i-1x} \\ P_{i-1y} + \lambda_i\,\ell_{i-1y} \\ P_{i-1z} + \lambda_i\,\ell_{i-1z} \\ 1 \end{bmatrix} = \bar{P}_{i-1} + \lambda_i\bar{\ell}_{i-1}, \tag{2.11}
$$

can be obtained by equating Eq. (2.7) to ${}^i\bar{P}_i = {}^i\bar{A}_0\,\bar{P}_i = ({}^0\bar{A}_i)^{-1}\bar{P}_i$. That is,

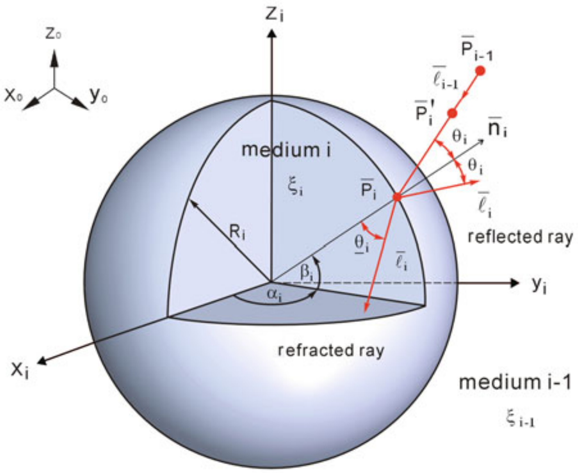

Fig. 2.4 Raytracing at spherical boundary surface $\bar{r}_i$

$$
\begin{aligned}
{}^{i}\bar{P}_i &= \begin{bmatrix} I_{ix} & I_{iy} & I_{iz} & -(I_{ix}t_{ix} + I_{iy}t_{iy} + I_{iz}t_{iz}) \\ J_{ix} & J_{iy} & J_{iz} & -(J_{ix}t_{ix} + J_{iy}t_{iy} + J_{iz}t_{iz}) \\ K_{ix} & K_{iy} & K_{iz} & -(K_{ix}t_{ix} + K_{iy}t_{iy} + K_{iz}t_{iz}) \\ 0 & 0 & 0 & 1 \end{bmatrix} \begin{bmatrix} P_{i-1x} + \lambda_i\,\ell_{i-1x} \\ P_{i-1y} + \lambda_i\,\ell_{i-1y} \\ P_{i-1z} + \lambda_i\,\ell_{i-1z} \\ 1 \end{bmatrix} \\
&= \begin{bmatrix} \sigma_i \\ \rho_i \\ \tau_i \\ 1 \end{bmatrix} = {}^{i}\bar{r}_i = \begin{bmatrix} |R_i|\; C\beta_i C\alpha_i \\ |R_i|\; C\beta_i S\alpha_i \\ |R_i|\; S\beta_i \\ 1 \end{bmatrix},
\end{aligned}
\tag{2.12}
$$

where σ_i, ρ_i, and τ_i are coordinates of incidence point expressed in boundary coordinate frame $(xyz)_i$, given by

$$
\begin{aligned}
\sigma_i &= I_{ix}(P_{i-1x} + \ell_{i-1x}\lambda_i) + I_{iy}\left(P_{i-1y} + \ell_{i-1y}\lambda_i\right) \\
&\quad + I_{iz}(P_{i-1z} + \ell_{i-1z}\lambda_i) - (I_{ix}t_{ix} + I_{iy}t_{iy} + I_{iz}t_{iz}) \\
&= I_{ix}P_{ix} + I_{iy}P_{iy} + I_{iz}P_{iz} - (I_{ix}t_{ix} + I_{iy}t_{iy} + I_{iz}t_{iz}),
\end{aligned}
\tag{2.13}
$$

$$
\begin{aligned}
\rho_i &= J_{ix}(P_{i-1x} + \ell_{i-1x}\lambda_i) + J_{iy}\left(P_{i-1y} + \ell_{i-1y}\lambda_i\right) \\
&\quad + J_{iz}(P_{i-1z} + \ell_{i-1z}\lambda_i) - (J_{ix}t_{ix} + J_{iy}t_{iy} + J_{iz}t_{iz}) \\
&= J_{ix}P_{ix} + J_{iy}P_{iy} + J_{iz}P_{iz} - (J_{ix}t_{ix} + J_{iy}t_{iy} + J_{iz}t_{iz}),
\end{aligned}
\tag{2.14}
$$

$$
\begin{aligned}
\tau_i &= K_{ix}(P_{i-1x} + \ell_{i-1x}\lambda_i) + K_{iy}\left(P_{i-1y} + \ell_{i-1y}\lambda_i\right) \\
&\quad + K_{iz}(P_{i-1z} + \ell_{i-1z}\lambda_i) - (K_{ix}t_{ix} + K_{iy}t_{iy} + K_{iz}t_{iz}) \\
&= K_{ix}P_{ix} + K_{iy}P_{iy} + K_{iz}P_{iz} - (K_{ix}t_{ix} + K_{iy}t_{iy} + K_{iz}t_{iz}).
\end{aligned}
\tag{2.15}
$$

From the sum of σ_i^2, ρ_i^2 and τ_i^2, λ_i is obtained as

$$
\lambda_i = -D_i \pm \sqrt{D_i^2 - E_i}, \tag{2.16}
$$

where

$$
D_i = \ell_{i-1x}(P_{i-1x} - t_{ix}) + \ell_{i-1y}(P_{i-1y} - t_{iy}) + \ell_{i-1z}(P_{i-1z} - t_{iz}), \tag{2.17}
$$

$$
E_i = P_{i-1x}^2 + P_{i-1y}^2 + P_{i-1z}^2 - R_i^2 + t_{ix}^2 + t_{iy}^2 + t_{iz}^2 - 2(t_{ix}P_{i-1x} + t_{iy}P_{i-1y} + t_{iz}P_{i-1z}). \tag{2.18}
$$

The non-negative parameter λ_i represents the geometrical path length from point $\bar{P}_{i-1}$ to point $\bar{P}_i$. Also note that the $\pm$ sign in Eq. (2.16) indicates the two possible intersection points of the ray with a complete sphere. More specifically, $\lambda_i = -D_i - \sqrt{D_i^2 - E_i}$ refers to the nearer intersection point while $\lambda_i = -D_i + \sqrt{D_i^2 - E_i}$ refers to the further point. Clearly, only one of these points is useful in practical systems, and thus the appropriate sign must be chosen. When $\rho_i^2 + \sigma_i^2 \neq 0$, α_i $(0 \leq \alpha_i < 2\pi)$ and β_i $(-\pi/2 \leq \beta_i \leq \pi/2)$ at the incidence point $\bar{P}_i$ can be solved from the following equations:

$$
\alpha_i = \mathrm{atan2}(\rho_i, \sigma_i), \tag{2.19}
$$

$$
\beta_i = \mathrm{atan2}(\tau_i, \sqrt{\sigma_i^2 + \rho_i^2}). \tag{2.20}
$$

It is noted from the third component of Eq. (2.12) that β_i can also be determined as $\beta_i = \arcsin(\tau_i/|R_i|)$. However, β_i cannot be obtained using this equation when the incoming ray $\bar{R}_{i-1}$ does not intersect with the complete sphere of $\bar{r}_i$ when $|R_i| < |\tau_i|$. Notably, Eq. (2.20) avoids this problem since it always yields a solution provided that $\sigma_i^2 + \rho_i^2 + \tau_i^2 \neq 0$.

The points located at $\beta_i = \pm\pi/2$ on a spherical boundary surface are pseudo-singular points (or irregular points), at which $\partial^i\bar{r}_i/\partial\beta_i$ and $\partial^i\bar{r}_i/\partial\alpha_i$ are not linearly independent. As a result, the cross product $\partial^i\bar{r}_i/\partial\beta_i \times \partial^i\bar{r}_i/\partial\alpha_i$ cannot be performed. To avoid this problem, an assumption is made throughout this book that the y_i axis of the spherical boundary surface always coincides with the optical axis of the system.

2.2.3 Unit Directional Vectors of Reflected and Refracted Rays

To trace a reflected or refracted ray at the current boundary surface $\bar{r}_i$, the incidence angle θ_i (defined in geometrical optics as a non-obtuse angle, i.e., $0° \le \theta_i \le 90°$) must first be known. In practice, $C\theta_i$ is determined via the dot product of $\bar{\ell}_{i-1}$ and $\bar{n}_i$, i.e., $C\theta_i = \left|\bar{\ell}_{i-1} \cdot \bar{n}_i\right|$ (Figs. 2.5 and 2.6). For every incidence point, there exist two possible unit normal vectors, and thus for each particular application, it is necessary to choose the correct one (referred to hereafter as the active unit normal vector, $\bar{n}_i$). By default, this book always chooses the active unit normal vector which forms an obtuse angle $90° < \eta < 180°$ with $\bar{\ell}_{i-1}$. Consequently,$C\theta_i$ can be computed without the absolute symbol as

$$
\begin{aligned}
C\theta_i &= -\bar{\ell}_{i-1} \cdot \bar{n}_i = -\left(\ell_{i-1x} n_{ix} + \ell_{i-1y} n_{iy} + \ell_{i-1z} n_{iz}\right) \\
&= -s_i\left[\ell_{i-1x}(I_{ix}C\beta_iC\alpha_i + J_{ix}C\beta_iS\alpha_i + K_{ix}S\beta_i) + \ell_{i-1y}\left(I_{iy}C\beta_iC\alpha_i + J_{iy}C\beta_iS\alpha_i + K_{iy}S\beta_i\right)\right. \\
&\quad \left. + \ell_{i-1z}(I_{iz}C\beta_iC\alpha_i + J_{iz}C\beta_iS\alpha_i + K_{iz}S\beta_i)\right].
\end{aligned}
\tag{2.21}
$$

Fig. 2.5 Reflected unit directional vector obtained by rotating active unit normal vector $\bar{n}_i$ about $\bar{m}_i$ by angle θ_i

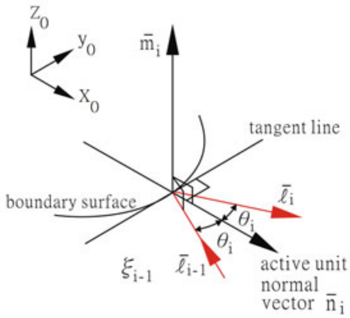

Fig. 2.6 Refracted unit directional vector obtained by rotating active unit normal vector $\bar{n}_i$ about $\bar{m}_i$ by angle $\pi - \underline{\theta}_i$

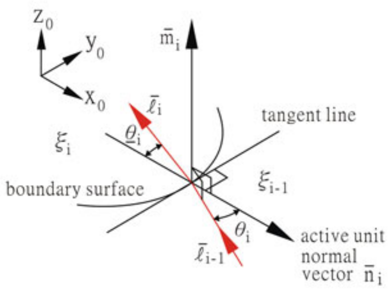

The refraction angle $\underline{\theta}_i$ between two optical media satisfies Snell's law, that is

$$S\underline{\theta}_i = \frac{\xi_{i-1}}{\xi_i} S\theta_i = N_i S\theta_i, \tag{2.22}$$

where ξ_i is the refractive index of medium i and $N_i = \xi_{i-1}/\xi_i$ is the refractive index of medium $i-1$ relative to that of medium i. Total internal reflection is a phenomenon that the ray will not cross the boundary and instead be totally reflected back internally. It happens when a ray strikes the boundary surface at an incident angle θ_i larger than the critical angle $\theta_{i/critical}$ (where $S\theta_{i/critical} = N_i$) if $\xi_i < \xi_{i-1}$.

To trace the reflected or refracted ray at the boundary surface, the common unit normal vector $\bar{m}_i$ of the active unit normal vector $\bar{n}_i$ and $\bar{\ell}_{i-1}$ (see Fig. 2.5) is required, i.e.,

$$\bar{m}_i = \begin{bmatrix} m_{ix} & m_{iy} & m_{iz} & 0 \end{bmatrix}^T = \frac{\bar{n}_i \times \bar{\ell}_{i-1}}{S\theta_i}. \tag{2.23}$$

It is useful to have the following equation, which is derived from Eq. (2.23), when we determine the unit directional vectors $\bar{\ell}_i$ of the reflected and refracted rays:

$$S\theta_i(\bar{m}_i \times \bar{n}_i) = (\bar{n}_i \times \bar{\ell}_{i-1}) \times \bar{n}_i = \bar{\ell}_{i-1} - (\bar{n}_i \cdot \bar{\ell}_{i-1})\bar{n}_i = \bar{\ell}_{i-1} + \bar{n}_i\, C\theta_i. \tag{2.24}$$

According to the reflection law of optics, the reflected unit directional vector $\bar{\ell}_i$ can be obtained by rotating the active unit normal vector $\bar{n}_i$ about $\bar{m}_i$ through an angle θ_i (Fig. 2.5 and Eq. (1.25)). In other words, $\bar{\ell}_i$ is obtained as

$$\begin{aligned}\bar{\ell}_i &= \begin{bmatrix} \ell_{ix} & \ell_{iy} & \ell_{iz} & 0 \end{bmatrix}^T = \mathrm{rot}(\bar{m}_i, \theta_i)\bar{n}_i \\ &= \begin{bmatrix} m_{ix}^2(1-C\theta_i)+C\theta_i & m_{iy}m_{ix}(1-C\theta_i)-m_{iz}S\theta_i & m_{iz}m_{ix}(1-C\theta_i)+m_{iy}S\theta_i & 0 \\ m_{ix}m_{iy}(1-C\theta_i)+m_{iz}S\theta_i & m_{iy}^2(1-C\theta_i)+C\theta_i & m_{iz}m_{iy}(1-C\theta_i)-m_{ix}S\theta_i & 0 \\ m_{ix}m_{iz}(1-C\theta_i)-m_{iy}S\theta_i & m_{iy}m_{iz}(1-C\theta_i)+m_{ix}S\theta_i & m_{iz}^2(1-C\theta_i)+C\theta_i & 0 \\ 0 & 0 & 0 & 1 \end{bmatrix} \\ &\quad \begin{bmatrix} n_{ix} \\ n_{iy} \\ n_{iz} \\ 0 \end{bmatrix}.\end{aligned} \tag{2.25}$$

Further simplification of Eq. (2.25) is possible by utilizing Eq. (2.24), resulting in

$$\bar{\ell}_i = \begin{bmatrix} \ell_{ix} \\ \ell_{iy} \\ \ell_{iz} \\ 0 \end{bmatrix} = \begin{bmatrix} \ell_{i-1x} + 2C\theta_i\, n_{ix} \\ \ell_{i-1y} + 2C\theta_i\, n_{iy} \\ \ell_{i-1z} + 2C\theta_i\, n_{iz} \\ 0 \end{bmatrix} = \bar{\ell}_{i-1} + 2C\theta_i\, \bar{n}_i. \tag{2.26}$$

Notably, $\bar{\ell}_i$ can also be obtained by rotating $\bar{\ell}_{i-1}$ about $\bar{m}_i$ through an angle $\pi + 2\theta_i$, i.e.,

$$\bar{\ell}_i = \mathrm{rot}(\bar{m}_i, \pi + 2\theta_i)\bar{\ell}_{i-1}. \tag{2.27}$$

According to the refraction law of optics, the refracted unit directional vector $\bar{\ell}_i$ can be obtained by rotating the active unit normal vector $\bar{n}_i$ about $\bar{m}_i$ through an angle $\pi - \underline{\theta}_i$ (Fig. 2.6), i.e.,

$$\begin{aligned}\bar{\ell}_i &= [\,\ell_{ix} \quad \ell_{iy} \quad \ell_{iz} \quad 0\,]^T = \mathrm{rot}(\bar{m}_i, \pi - \underline{\theta}_i)\bar{n}_i \\ &= \begin{bmatrix} m_{ix}^2(1 + C\underline{\theta}_i) - C\underline{\theta}_i & m_{iy}m_{ix}(1 + C\underline{\theta}_i) - m_{iz}S\underline{\theta}_i & m_{iz}m_{ix}(1 + C\underline{\theta}_i) + m_{iy}S\underline{\theta}_i & 0 \\ m_{ix}m_{iy}(1 + C\underline{\theta}_i) + m_{iz}S\underline{\theta}_i & m_{iy}^2(1 + C\underline{\theta}_i) - C\underline{\theta}_i & m_{iz}m_{iy}(1 + C\underline{\theta}_i) - m_{ix}S\underline{\theta}_i & 0 \\ m_{ix}m_{iz}(1 + C\underline{\theta}_i) - m_{iy}S\underline{\theta}_i & m_{iy}m_{iz}(1 + C\underline{\theta}_i) + m_{ix}S\underline{\theta}_i & m_{iz}^2(1 + C\underline{\theta}_i) - C\underline{\theta}_i & 0 \\ 0 & 0 & 0 & 1 \end{bmatrix} \\ &\quad \begin{bmatrix} n_{ix} \\ n_{iy} \\ n_{iz} \\ 0 \end{bmatrix}.\end{aligned} \tag{2.28}$$

Again, further simplification of Eq. (2.28) is possible by utilizing Eq. (2.24) and Snell's law, $S\underline{\theta}_i = N_i S\theta_i$. The following refracted unit directional vector $\bar{\ell}_i$ is thus obtained:

$$\begin{aligned}\bar{\ell}_i = \begin{bmatrix} \ell_{ix} \\ \ell_{iy} \\ \ell_{iz} \\ 0 \end{bmatrix} &= \begin{bmatrix} \left(-\sqrt{1 - N_i^2 + (N_i C\theta_i)^2}\right) n_{ix} + N_i(\ell_{i-1x} + C\theta_i\ n_{ix}) \\ \left(-\sqrt{1 - N_i^2 + (N_i C\theta_i)^2}\right) n_{iy} + N_i(\ell_{i-1y} + C\theta_i\ n_{iy}) \\ \left(-\sqrt{1 - N_i^2 + (N_i C\theta_i)^2}\right) n_{iz} + N_i(\ell_{i-1z} + C\theta_i\ n_{iz}) \\ 0 \end{bmatrix} \\ &= \left(-\sqrt{1 - N_i^2 + (N_i C\theta_i)^2}\right)\bar{n}_i + N_i\left(\bar{\ell}_{i-1} + C\theta_i \bar{n}_i\right),\end{aligned} \tag{2.29}$$

where $\bar{n}_i = [\,n_{ix} \quad n_{iy} \quad n_{iz} \quad 0\,]^T$ and $C\theta_i$ are given by Eqs. (2.10) and (2.21), respectively. Of course, the refracted unit directional vector $\bar{\ell}_i$ can also be determined by rotating $\bar{\ell}_{i-1}$ about $\bar{m}_i$ through an angle $\pi - \underline{\theta}_i + \theta_i$, i.e., $\bar{\ell}_i = \mathrm{rot}(\bar{m}_i, \pi - \underline{\theta}_i + \theta_i)\bar{\ell}_{i-1}$.

It is important to point out that total internal reflection occurs when $1 - N_i^2 + (N_i C\theta_i)^2 < 0$.

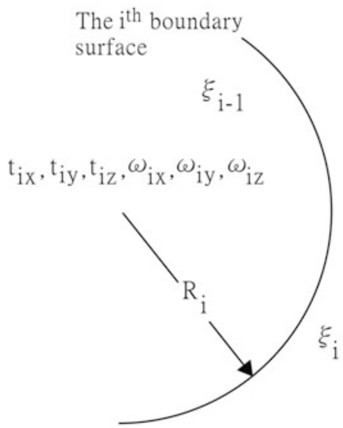

Fig. 2.7 Boundary variables of spherical boundary surface

Referring to Fig. 2.7, designate

$$\bar{X}_i = [\, t_{ix} \quad t_{iy} \quad t_{iz} \quad \omega_{ix} \quad \omega_{iy} \quad \omega_{iz} \quad \xi_{i-1} \quad \xi_i \quad R_i \,]^T \tag{2.30}$$

as the boundary variable vector of a spherical boundary surface, where this vector comprises the six pose variables of Eq. (2.9), the refractive indices ξ_{i-1} and ξ_i, and the radius R_i of the boundary surface.

It is noted from Eqs. (2.11), (2.26) and (2.29) that the ray $\bar{R}_i$ is a function of the incoming ray $\bar{R}_{i-1}$ with the given source ray $\bar{R}_0$ (Fig. 2.8). In other words, $\bar{R}_i$ is a recursive function, i.e., a function which operates in turn on another function (or functions). It is like a Russian nesting doll. Each doll has a smaller and smaller doll inside it. To evaluate a recursive function, it is first necessary to evaluate the internal functions, and to then determine the outer function based on the results of these internal functions.

Example 2.1 The raytracing equations for a meridional ray traveling through an axis-symmetrical system can be obtained by setting the x_0 components of Eqs. (2.11), (2.26) and (2.29) to zero. However, in the following, these equations are derived independently for the system shown in Fig. 2.9, in which a spherical

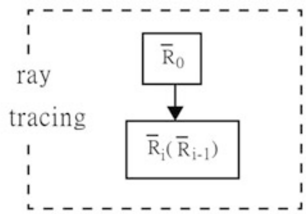

Fig. 2.8 Ray $\bar{R}_i$ is function of incoming ray $\bar{R}_{i-1}$ by given source ray $\bar{R}_0$

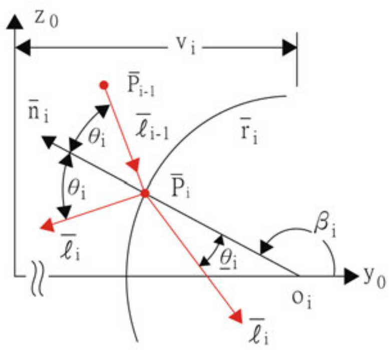

Fig. 2.9 Tracing meridional ray at spherical boundary surface in axis-symmetrical system

boundary surface $\bar{r}_i = [0 \quad |R_i|C\beta_i + v_i \quad |R_i|S\beta_i \quad 1]^T$ with center o_i is located at point $y_0 = v_i$ along the optical axis of an axis-symmetrical system. Assume that a meridional ray $\bar{R}_{i-1}$ originating at point $\bar{P}_{i-1} = [0 \quad P_{i-1y} \quad P_{i-1z} \quad 1]^T$ and directed along $\bar{\ell}_{i-1} = [0 \quad \ell_{i-1y} \quad \ell_{i-1z} \quad 0]^T$ ($\ell_{i-1y}^2 + \ell_{i-1z}^2 = 1$ with $0 < \ell_{i-1y}$ and $\ell_{i-1z} < 0$) is reflected or refracted at boundary surface $\bar{r}_i$. The incidence point $\bar{P}_i$ at which the ray strikes $\bar{r}_i$ is given by

$$\bar{P}_i = \begin{bmatrix} 0 \\ P_{iy} \\ P_{iz} \\ 1 \end{bmatrix} = \bar{P}_{i-1} + \lambda_i \bar{\ell}_{i-1} = \begin{bmatrix} 0 \\ P_{i-1y} + \lambda_i \ell_{i-1y} \\ P_{i-1z} + \lambda_i \ell_{i-1z} \\ 1 \end{bmatrix},$$

where the parameter λ_i is obtained by setting $\bar{P}_i = \bar{r}_i$, yielding $\lambda_i = -D_i \pm \sqrt{D_i^2 - E_i}$, with $D_i = \ell_{i-1y}(P_{i-1y} - v_i) + \ell_{i-1z}P_{i-1z}$ and $E_i = (P_{i-1y} - v_i)^2 + P_{i-1z}^2 - R_i^2$.

Since the active unit normal vector is $\bar{n}_i = [0 \quad C\beta_i \quad S\beta_i \quad 0]^T$, the incidence angle θ_i can be computed as

$$C\theta_i = \left|\bar{\ell}_{i-1} \cdot \bar{n}_i\right| = \left|\bar{\ell}_{i-1}^T \bar{n}_i\right| = (-\bar{\ell}_{i-1}) \cdot \bar{n}_i = -(\ell_{i-1y}C\beta_i + \ell_{i-1z}S\beta_i).$$

It is noted from Fig. 2.9 that the reflected unit directional vector $\bar{\ell}_i$ can be obtained by rotating the active unit normal vector $\bar{n}_i$ about the x_0 axis through an angle θ_i. Thus, the reflected unit directional vector $\bar{\ell}_i$ is obtained as

$$\bar{\ell}_i = \begin{bmatrix} 0 \\ \ell_{iy} \\ \ell_{iz} \\ 0 \end{bmatrix} = \text{rot}(\bar{x}, \theta_i)\bar{n}_i = \begin{bmatrix} 0 \\ C(\theta_i + \beta_i) \\ S(\theta_i + \beta_i) \\ 0 \end{bmatrix}.$$

According to the refraction law of optics, the refracted unit directional vector $\bar{\ell}_i$ can be obtained by rotating the active unit normal vector $\bar{n}_i$ about the x_0 axis through an angle $\pi - \underline{\theta}_i$. In other words,

$$\bar{\ell}_i = \begin{bmatrix} 0 \\ \ell_{iy} \\ \ell_{iz} \\ 0 \end{bmatrix} = \mathrm{rot}(\bar{x}, \pi - \underline{\theta}_i)\bar{n}_i = \begin{bmatrix} 0 \\ -C(\underline{\theta}_i - \beta_i) \\ S(\underline{\theta}_i - \beta_i) \\ 0 \end{bmatrix},$$

where the refraction angle $\underline{\theta}_i$ satisfies Snell's law, i.e., $S\underline{\theta}_i = (\xi_{i-1}/\xi_i)S\theta_i = N_i S\theta_i$.

It is noted that for the case where the source ray $\bar{R}_{i-1}$ travels in the upward direction (i.e., $0 < \ell_{i-1z}$), the unit directional vectors of the reflected and refracted rays are determined as $\bar{\ell}_i = \mathrm{rot}(-\bar{x}, \theta_i)\bar{n}_i$ and $\bar{\ell}_i = \mathrm{rot}(-\bar{x}, \pi - \underline{\theta}_i)\bar{n}_i$, respectively. The example above shows that the raytracing equations for a meridional ray traveling through an axis-symmetrical system can be easily obtained. However, caution should be exercised when applying the rotation matrix since the rotation axis depends on both $\bar{\ell}_{i-1}$ and the active unit normal vector $\bar{n}_i$ (see Eq. (2.23)).

Example 2.2 Skew-ray tracing in any element containing spherical boundary surfaces is comparatively difficult. As a result, only numerical examples are provided here for illustration purposes. Consider the bi-convex element shown in Fig. 2.10, with $v_1 = 5$, thickness $q_{e1} = 10$, refractive index $\xi_{e1} = 1.5$, and surface radii $R_1 = 50$ and $R_2 = -100$. (1) Assign boundary coordinate frames $(xyz)_1$ and $(xyz)_2$ to the two spherical boundary surfaces, $\bar{r}_1$ and $\bar{r}_2$. (2) Find the unit normal vectors ${}^1\bar{n}_1$ and ${}^2\bar{n}_2$. (3) Determine the pose matrix ${}^0\bar{A}_1$ and boundary variable vector $\bar{X}_1$. (4) Assign the pose matrix ${}^0\bar{A}_2$ and determine boundary variable vector $\bar{X}_2$. (5) Find the unit normal vectors $\bar{n}_1$ and $\bar{n}_2$. (6) Write out the source ray $\bar{R}_0$ when $\bar{P}_0 = [0 \quad -5 \quad 5 \quad 1]^T$ and $\alpha_0 = 0°$, $\beta_0 = 5°$. (7) Find λ_1, α_1, β_1, unit normal vectors $\bar{n}_1$, the value of s_1 for the active unit normal vector, the incidence angle θ_1, the refractive index N_1, and the refracted ray $\bar{R}_1$ when ray $\bar{R}_0$ is refracted at the first boundary surface, $\bar{r}_1$. (8) Find λ_2, α_2, β_2, unit normal vectors $\bar{n}_2$, the value of s_2 for the active unit normal vector, the incidence angle θ_1, the refractive index N_2, and the refracted ray $\bar{R}_2$ when ray $\bar{R}_1$ is refracted at the second boundary surface, $\bar{r}_2$.

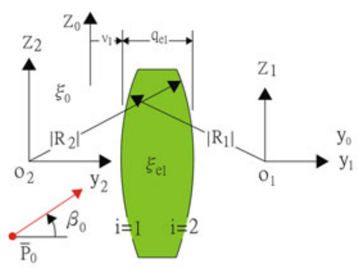

Fig. 2.10 Assigned coordinate frames $(xyz)_1$ and $(xyz)_2$ for bi-convex lens

Solution

(1) The assigned coordinate frames $(xyz)_1$ and $(xyz)_2$ are shown in Fig. 2.10. Note that their origins, o_1 and o_2, are located at the centers of $\bar{r}_1$ and $\bar{r}_2$, respectively, while the y_1 and y_2 axes coincide with the y_0 axis.

(2) ${}^1\bar{n}_1 = s_1[C\beta_1 C\alpha_1 \quad C\beta_1 S\alpha_1 \quad S\beta_1 \quad 0]^T$,
${}^2\bar{n}_2 = s_2[C\beta_2 C\alpha_2 \quad C\beta_2 S\alpha_2 \quad S\beta_2 \quad 0]^T$.

(3) $${}^0\bar{A}_1 = \text{tran}(0, v_1 + R_1, 0) = \text{tran}(0, 5 + 50, 0) = \begin{bmatrix} 1 & 0 & 0 & 0 \\ 0 & 1 & 0 & 55 \\ 0 & 0 & 1 & 0 \\ 0 & 0 & 0 & 1 \end{bmatrix},$$

$$\bar{X}_1 = [t_{1x} \quad v_1 + R_1 \quad t_{1z} \quad \omega_{1x} \quad \omega_{1y} \quad \omega_{1z} \quad \xi_0 \quad \xi_1 \quad R_1]^T$$
$$= [0 \quad 55 \quad 0 \quad 0 \quad 0 \quad 0 \quad 1 \quad 1.5 \quad 50]^T.$$

(4) $${}^0\bar{A}_2 = \text{tran}(0, v_1 + q_{e1} + R_2, 0) = \text{tran}(0, 5 + 10 - 100, 0)$$
$$= \begin{bmatrix} 1 & 0 & 0 & 0 \\ 0 & 1 & 0 & -85 \\ 0 & 0 & 1 & 0 \\ 0 & 0 & 0 & 1 \end{bmatrix},$$

$$\bar{X}_2 = [t_{2x} \quad v_1 + q_{e1} + R_2 \quad t_{2z} \quad \omega_{2x} \quad \omega_{2y} \quad \omega_{2z} \quad \xi_1 \quad \xi_2 \quad R_2]^T$$
$$= [0 \quad -85 \quad 0 \quad 0 \quad 0 \quad 0 \quad 1.5 \quad 1 \quad -100]^T.$$

(5) The two unit normal vectors of $\bar{r}_1$ are given as $\bar{n}_1 = {}^0\bar{A}_1\,{}^1\bar{n}_1 = s_1[C\beta_1 C\alpha_1 \quad C\beta_1 S\alpha_1 \quad S\beta_1 \quad 0]^T$. Similarly, the unit normal vectors of $\bar{r}_2$ are given as $\bar{n}_2 = {}^0\bar{A}_2\,{}^2\bar{n}_2 = s_2[C\beta_2 C\alpha_2 \quad C\beta_2 S\alpha_2 \quad S\beta_2 \quad 0]^T$.

(6) $\bar{R}_0 = [0 \quad -5 \quad 5 \quad C5°C90° \quad C5°S90° \quad S5°]^T$.

(7) $\lambda_1 = 10.38951$,
$\alpha_1 = -90°$,
$\beta_1 = 6.78304°$.
The active unit normal vector of $\bar{r}_1$ is $\bar{n}_1 = [C\beta_1 C\alpha_1 \quad C\beta_1 S\alpha_1 \quad S\beta_1 \quad 0]^T$, leading to $s_1 = 1$,
$\theta_1 = 11.78304°$,
$N_1 = \xi_0/\xi_1 = 1/1.5$,
$\bar{R}_1 = [0 \quad 5.34997 \quad 5.90551 \quad 0 \quad 0.99983 \quad 0.01817]^T$.

(8) $\lambda_2 = 9.46673$,
$\alpha_2 = 90°$,
$\beta_2 = 3.48433°$.
The active unit normal vector of $\bar{r}_2$ is $\bar{n}_2 = [-C\beta_2 C\alpha_2 \quad -C\beta_2 S\alpha_2 - S\beta_2 \quad 0]^T$, leading to $s_2 = -1$,
$\theta_2 = 2.44297°$,
$N_2 = \xi_1/\xi_2 = 1.5$,
$\bar{R}_2 = [0 \quad 14.81515 \quad 6.07756 \quad 0 \quad 0.99999 \quad -0.00317]^T$.

2.3 Flat Boundary Surfaces

Many optical systems contain elements with flat boundary surfaces. Typical examples include plano-convex lenses, plano-concave lenses, optical flats, beam-splitters, and flat first-surface mirrors. Raytracing at a flat boundary surface is thus of great practical interest. Most studies treat flat boundary surfaces as a spherical surface with zero curvature (e.g., p. 312 of [34]). However, certain ray-tracing equations for prisms cannot be obtained using such an approach. Accordingly, a more different methodology for dealing with flat boundary surfaces is required.

2.3.1 Flat Boundary Surface and Associated Unit Normal Vector

As stated in Sect. 2.2, the y_i axis of boundary coordinate frame $(xyz)_i$ in an axis-symmetrical optical system is assumed to coincide with the optical axis of the system. If β_i is the length parameter along y_i axis measured from the origin of $(xyz)_i$, a flat boundary surface can be obtained simply by rotating its generating line (Fig. 2.11)

$$ {}^{i}\bar{q}_i = \begin{bmatrix} 0 \\ 0 \\ \beta_i \\ 1 \end{bmatrix} (0 \le \beta_i) \tag{2.31} $$

about the y_i axis through an angle α_i $(0 \le \alpha_i < 2\pi)$, i.e.,

$$ {}^{i}\bar{r}_i = \begin{bmatrix} x_i \\ y_i \\ z_i \\ 1 \end{bmatrix} = \mathrm{rot}(\bar{y}, \alpha_i)\,{}^{i}\bar{q}_i = \begin{bmatrix} C\alpha_i & 0 & S\alpha_i & 0 \\ 0 & 1 & 0 & 0 \\ -S\alpha_i & 0 & C\alpha_i & 0 \\ 0 & 0 & 0 & 1 \end{bmatrix} \begin{bmatrix} 0 \\ 0 \\ \beta_i \\ 1 \end{bmatrix} = \begin{bmatrix} \beta_i S\alpha_i \\ 0 \\ \beta_i C\alpha_i \\ 1 \end{bmatrix}. \tag{2.32} $$

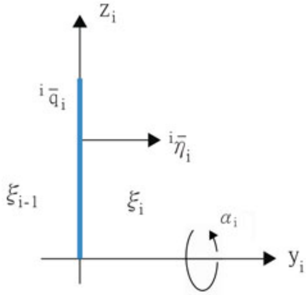

Fig. 2.11 Generating line and associated unit normal vector of flat boundary surface

The two possible unit normal vectors ${}^{i}\bar{\eta}_i$ of the generating curve ${}^{i}\bar{q}_i$ are given by

$$
{}^{i}\bar{\eta}_i = \begin{bmatrix} \eta_{ix} \\ \eta_{iy} \\ \eta_{iz} \\ 0 \end{bmatrix} = s_i \begin{bmatrix} 0 \\ -1 \\ 0 \\ 0 \end{bmatrix}, \tag{2.33}
$$

where, again, s_i is set to +1 or −1 to show that there exist two possible unit normal vectors pointing in opposite directions from one another. The unit normal vectors ${}^{i}\bar{n}_i$ of boundary surface ${}^{i}\bar{r}_i$ are then determined by rotating ${}^{i}\bar{\eta}_i$ about the y_i axis through an angle α_i, i.e.,

$$
{}^{i}\bar{n}_i = \mathrm{rot}(\bar{y}, \alpha_i)\,{}^{i}\bar{\eta}_i = s_i \begin{bmatrix} C\alpha_i & 0 & s\alpha_i & 0 \\ 0 & 1 & 0 & 0 \\ -S\alpha_i & 0 & C\alpha_i & 0 \\ 0 & 0 & 0 & 1 \end{bmatrix} \begin{bmatrix} 0 \\ -1 \\ 0 \\ 0 \end{bmatrix} = s_i \begin{bmatrix} 0 \\ -1 \\ 0 \\ 0 \end{bmatrix}. \tag{2.34}
$$

Equations (2.32) and (2.34) describe the flat boundary surface ${}^{i}\bar{r}_i$ and its unit normal vector ${}^{i}\bar{n}_i$ with respect to the boundary coordinate frame $(xyz)_i$. However, as discussed earlier, many derivations in this book are built relative to the world coordinate frame $(xyz)_o$. The following pose matrix of frame $(xyz)_i$ with respect to $(xyz)_0$ is thus required:

$$
\begin{aligned}
{}^{0}\bar{A}_i &= \mathrm{tran}(t_{ix}, 0, 0)\mathrm{tran}(0, t_{iy}, 0)\mathrm{tran}(0, 0, t_{iz})\mathrm{rot}(\bar{z}, \omega_{iz})\mathrm{rot}(\bar{y}, \omega_{iy})\mathrm{rot}(\bar{x}, \omega_{ix}) \\
&= \begin{bmatrix} C\omega_{iz}C\omega_{iy} & C\omega_{iz}S\omega_{iy}S\omega_{ix} - S\omega_{iz}C\omega_{ix} & C\omega_{iz}S\omega_{iy}C\omega_{ix} + S\omega_{iz}S\omega_{ix} & t_{ix} \\ S\omega_{iz}C\omega_{iy} & S\omega_{iz}S\omega_{iy}S\omega_{ix} + C\omega_{iz}C\omega_{ix} & S\omega_{iz}S\omega_{iy}C\omega_{ix} - C\omega_{iz}S\omega_{ix} & t_{iy} \\ -S\omega_{iy} & C\omega_{iy}S\omega_{ix} & C\omega_{iy}C\omega_{ix} & t_{iz} \\ 0 & 0 & 0 & 1 \end{bmatrix} \\
&= \begin{bmatrix} I_{ix} & J_{ix} & K_{ix} & t_{ix} \\ I_{iy} & J_{iy} & K_{iy} & t_{iy} \\ I_{iz} & J_{iz} & K_{iz} & t_{iz} \\ 0 & 0 & 0 & 1 \end{bmatrix},
\end{aligned} \tag{2.35}
$$

where $t_{ix}, t_{iy}, t_{iz}, \omega_{ix}, \omega_{iy}$ and ω_{iz} are the pose variables of the flat boundary surface. The unit normal vector $\bar{n}_i$ can then be obtained with respect to $(xyz)_0$ as

$$
\bar{n}_i = \begin{bmatrix} n_{ix} \\ n_{iy} \\ n_{iz} \\ 0 \end{bmatrix} = {}^{0}\bar{A}_i\,{}^{i}\bar{n}_i = s_i \begin{bmatrix} I_{ix} & J_{ix} & K_{ix} & t_{ix} \\ I_{iy} & J_{iy} & K_{iy} & t_{iy} \\ I_{iz} & J_{iz} & K_{iz} & t_{iz} \\ 0 & 0 & 0 & 1 \end{bmatrix} \begin{bmatrix} 0 \\ -1 \\ 0 \\ 0 \end{bmatrix} = -s_i \begin{bmatrix} J_{ix} \\ J_{iy} \\ J_{iz} \\ 0 \end{bmatrix}. \tag{2.36}
$$

2.3.2 Incidence Point

Assume in Fig. 2.12 that a ray originating at point $\bar{P}_{i-1}$ on the previous boundary surface $\bar{r}_{i-1}$ is directed along the unit directional vector $\bar{\ell}_{i-1}$ and is reflected or refracted at current flat boundary surface $\bar{r}_i$. Any intermediate point $\bar{P}'_{i-1}$ lying along this ray as it travels from $\bar{P}_{i-1}$ is given by $\bar{P}'_{i-1} = \bar{P}_{i-1} + \lambda\bar{\ell}_{i-1}$. Moreover, the incidence point $\bar{P}_i$ at which the ray hits the flat boundary surface is given by

$$\bar{P}_i = \begin{bmatrix} P_{ix} \\ P_{iy} \\ P_{iz} \\ 1 \end{bmatrix} = \begin{bmatrix} P_{i-1x} + \lambda_i \ell_{i-1x} \\ P_{i-1y} + \lambda_i \ell_{i-1y} \\ P_{i-1z} + \lambda_i \ell_{i-1z} \\ 1 \end{bmatrix} = \bar{P}_{i-1} + \lambda_i \bar{\ell}_{i-1}, \tag{2.37}$$

where the parameter λ_i can be obtained by equating Eq. (2.32) to ${}^i\bar{P}_i = {}^i\bar{A}_0\bar{P}_i = ({}^0\bar{A}_i)^{-1}\bar{P}_i$, i.e.,

$$\begin{aligned} {}^i\bar{P}_i &= \begin{bmatrix} I_{ix} & I_{iy} & I_{iz} & -(I_{ix}t_{ix} + I_{iy}t_{iy} + I_{iz}t_{iz}) \\ J_{ix} & J_{iy} & J_{iz} & -(J_{ix}t_{ix} + J_{iy}t_{iy} + J_{iz}t_{iz}) \\ K_{ix} & K_{iy} & K_{iz} & -(K_{ix}t_{ix} + K_{iy}t_{iy} + K_{iz}t_{iz}) \\ 0 & 0 & 0 & 1 \end{bmatrix} \begin{bmatrix} P_{i-1x} + \lambda_i \ell_{i-1x} \\ P_{i-1y} + \lambda_i \ell_{i-1y} \\ P_{i-1z} + \lambda_i \ell_{i-1z} \\ 1 \end{bmatrix} \\ &= \begin{bmatrix} \sigma_i \\ \rho_i \\ \tau_i \\ 1 \end{bmatrix} = {}^i\bar{r}_i = \begin{bmatrix} \beta_i S\alpha_i \\ 0 \\ \beta_i C\alpha_i \\ 1 \end{bmatrix}, \end{aligned} \tag{2.38}$$

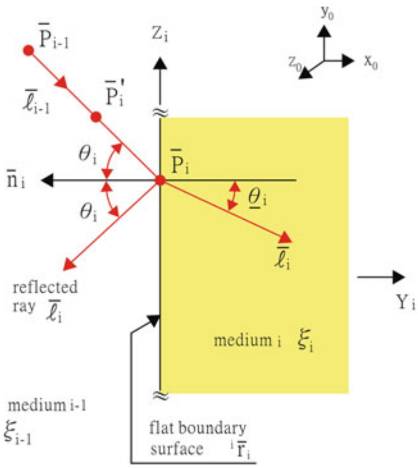

Fig. 2.12 Raytracing at flat boundary surface

in which σ_i, ρ_i and τ_i are given in Eqs. (2.13), (2.14) and (2.15), respectively. λ_i can be solved from the second component of Eq. (2.38) (i.e., $\rho_i = 0$) as

$$\lambda_i = \frac{-\left[J_{ix}P_{i-1x} + J_{iy}P_{i-1y} + J_{iz}P_{i-1z} - (J_{ix}t_{ix} + J_{iy}t_{iy} + J_{iz}t_{iz})\right]}{J_{ix}\ell_{i-1x} + J_{iy}\ell_{i-1y} + J_{iz}\ell_{i-1z}} = \frac{-D_i}{E_i}, \tag{2.39}$$

where

$$D_i = J_{ix}P_{i-1x} + J_{iy}P_{i-1y} + J_{iz}P_{i-1z} + e_i, \tag{2.40}$$

$$E_i = J_{ix}\ell_{i-1x} + J_{iy}\ell_{i-1y} + J_{iz}\ell_{i-1z}. \tag{2.41}$$

Note that parameter e_i in Eq. (2.40) is defined as $e_i = -(J_{ix}t_{ix} + J_{iy}t_{iy} + J_{iz}t_{iz})$ and is adopted in this book as a means of lumping six parameters together, thereby reducing the total number of variables to be considered. As discussed in Sect. (1.7, $-e_i$ represents the distance from the origin of coordinate frame $(xyz)_o$ to the origin of coordinate frame $(xyz)_i$ along the direction of the unit normal $\bar{n}_i$ (Fig. 1.16 with g = 0).

The parameters α_i $(0 \le \alpha_i < 2\pi)$ and β_i $(0 \le \beta_i)$, where incidence point $\bar{P}_i$ hits the $x_i z_i$ plane, are determined respectively by

$$\beta_i = \sqrt{\sigma_i^2 + \tau_i^2}, \tag{2.42}$$

$$\alpha_i \begin{cases} = \operatorname{atan2}(\sigma_i, \tau_i) & \text{when } \beta_i \ne 0 \\ = \text{any value} & \text{when } \beta_i = 0 \end{cases}. \tag{2.43}$$

Notably, even though the point at $\beta_i = 0$ of a flat boundary surface is a pseudo-singular point, it poses no computational problem.

2.3.3 *Unit Directional Vectors of Reflected and Refracted Rays*

The incidence angle θ_i, whose domain is $0^\circ \le \theta_i \le 90^\circ$, can be computed as $C\theta_i = \left|\bar{\ell}_{i-1} \cdot \bar{n}_i\right|$. Again, at every incidence point, there exist two possible unit normal vectors aligned in opposite directions to one another. To choose the correct unit normal vector, let the active unit normal vector $\bar{n}_i$ be once again defined as the vector possessing an obtuse angle $90^\circ < \eta < 180^\circ$ with $\bar{\ell}_{i-1}$. Having chosen the active unit normal vector $\bar{n}_i$, $C\theta_i$ can be computed without the absolute symbol as

$$C\theta_i = \left|\bar{\ell}_{i-1} \cdot \bar{n}_i\right| = -\bar{\ell}_{i-1} \cdot \bar{n}_i = s_i\left(J_{ix}\ell_{i-1x} + J_{iy}\ell_{i-1y} + J_{iz}\ell_{i-1z}\right) = s_i E_i. \quad (2.44)$$

The refraction angle $\underline{\theta}_i$ between two optical media must satisfy Snell's law, i.e., $S\underline{\theta}_i = (\xi_{i-1}/\xi_i)S\theta_i = N_i S\theta_i$. As for the case of a spherical boundary surface, the reflected unit directional vector $\bar{\ell}_i$ at a flat boundary surface can be obtained by rotating the active unit normal vector $\bar{n}_i$ about the unit common normal vector $\bar{m}_i$ (given in Eq. (2.23)) through an angle θ_i, yielding

$$\bar{\ell}_i = \begin{bmatrix} \ell_{ix} \\ \ell_{iy} \\ \ell_{iz} \\ 0 \end{bmatrix} = \begin{bmatrix} \ell_{i-1x} + 2C\theta_i\, n_{ix} \\ \ell_{i-1y} + 2C\theta_i\, n_{iy} \\ \ell_{i-1z} + 2C\theta_i\, n_{iz} \\ 0 \end{bmatrix} = \bar{\ell}_{i-1} + 2C\theta_i\, \bar{n}_i. \quad (2.45)$$

Similarly, the refracted unit directional vector $\bar{\ell}_i$ can be obtained by rotating the active unit normal vector $\bar{n}_i$ about the unit common vector $\bar{m}_i$ through an angle $\pi - \underline{\theta}_i$ (its detailed derivations were presented in Eq. (2.28)), giving

$$\bar{\ell}_i = \begin{bmatrix} \ell_{ix} \\ \ell_{iy} \\ \ell_{iz} \\ 0 \end{bmatrix} = \begin{bmatrix} -n_{ix}\sqrt{1 - N_i^2 + (N_i C\theta_i)^2} + N_i(\ell_{i-1x} + n_{ix}C\theta_i) \\ -n_{iy}\sqrt{1 - N_i^2 + (N_i C\theta_i)^2} + N_i(\ell_{i-1y} + n_{iy}C\theta_i) \\ -n_{iz}\sqrt{1 - N_i^2 + (N_i C\theta_i)^2} + N_i(\ell_{i-1z} + n_{iz}C\theta_i) \\ 0 \end{bmatrix}$$
$$= \left(N_i C\theta_i - \sqrt{1 - N_i^2 + (N_i C\theta_i)^2}\right)\bar{n}_i + N_i\bar{\ell}_{i-1}. \quad (2.46)$$

Note that total internal reflection occurs at this boundary surface when $1 - N_i^2 + (N_i C\,\theta_i)^2 < 0$.

It is noted from Eqs. (2.37), (2.45) and (2.46) that only six variables (i.e., $J_{ix}, J_{iy}, J_{iz}, e_i, \xi_{i-1}, \xi_i$) are needed to completely describe the effects of a flat boundary surface. The boundary variable vector of a flat boundary surface can thus be defined as

$$\bar{X}_i = [J_{ix} \quad J_{iy} \quad J_{iz} \quad e_i \quad \xi_{i-1} \quad \xi_i]^T. \quad (2.47)$$

It is noted that not all of the variables in $\bar{X}_i$ are independent since $J_{ix}^2 + J_{iy}^2 + J_{iz}^2 = 1$. Another example is $\xi_{i-1} = \xi_i$ for a reflective boundary surface. However, the inter-dependence of some of the components in $\bar{X}_i$ presents no computational difficulties if a system variable vector $\bar{X}_{sys}$ containing all of the independent variables of interest of the optical system is defined.

The discussions above consider the raytracing problem for a reflected or refracted ray $\bar{R}_i$ at a single boundary surface. However, the same approach can be applied successively to trace rays in an optical system containing n boundary

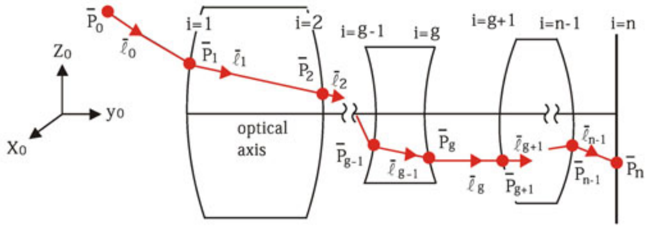

Fig. 2.13 Sequential tracing of ray $\bar{R}_g$ through optical system using proposed approach

surfaces. To trace a ray reflected or refracted at the gth boundary surface, it is first necessary to label the boundary surfaces of the system sequentially from 1 to n. The preceding raytracing methodology can then be applied sequentially with i = 1, i = 2, …, until i = g to obtain the ray $\bar{R}_g$ refracted or reflected at the gth boundary surface (see Fig. 2.13), where

$$\bar{P}_g = \begin{bmatrix} P_{gx} \\ P_{gy} \\ P_{gz} \\ 1 \end{bmatrix} = \begin{bmatrix} P_{g-1x} + \lambda_g \, \ell_{g-1x} \\ P_{g-1y} + \lambda_g \, \ell_{g-1y} \\ P_{g-1z} + \lambda_g \, \ell_{g-1z} \\ 1 \end{bmatrix} = \begin{bmatrix} P_{g-2x} + \lambda_{g-1} \, \ell_{g-2x} + \lambda_g \, \ell_{g-1x} \\ P_{g-2y} + \lambda_{g-1} \, \ell_{g-2y} + \lambda_g \, \ell_{g-1y} \\ P_{g-2z} + \lambda_{g-1} \, \ell_{g-2z} + \lambda_g \, \ell_{g-1z} \\ 1 \end{bmatrix} = \ldots$$
$$= \begin{bmatrix} P_{0x} + \lambda_1 \bar{\ell}_{0x} + \ldots + \lambda_g \bar{\ell}_{g-1x} \\ P_{0y} + \lambda_1 \bar{\ell}_{0y} + \ldots + \lambda_g \bar{\ell}_{g-1y} \\ P_{0z} + \lambda_1 \bar{\ell}_{0z} + \ldots + \lambda_g \bar{\ell}_{g-1z} \\ 1 \end{bmatrix} = \bar{P}_0 + \lambda_1 \bar{\ell}_0 + \ldots + \lambda_g \bar{\ell}_{g-1}. \tag{2.48}$$

Example 2.3 Skew-ray tracing in an optical element possessing only flat boundary surfaces is much simpler than in the case of an optical element containing spherical boundary surfaces. Consider the rectangular optical flat shown in Fig. 2.14 with separation v_1, thickness q_{e1}, and refractive index ξ_{e1}. (1) Assign boundary coordinate frames $(xyz)_1$ and $(xyz)_2$ to the two flat boundary surfaces, $\bar{r}_1$ and $\bar{r}_2$. (2) Find their unit normal vectors ${}^1\bar{n}_1$ and ${}^2\bar{n}_2$. (3) Determine the pose matrix ${}^0\bar{A}_1$ and boundary variable vector $\bar{X}_1$. (4) Assign the pose matrix ${}^0\bar{A}_2$ and determine boundary variable vector $\bar{X}_2$. (5) Find unit normal vectors $\bar{n}_1$, D_1, E_1, λ_1, β_1, α_1, $C\theta_1$, N_1, the value of s_1 for the active unit normal vector, and $\bar{\ell}_1$ when source ray $\bar{R}_0 = [0 \quad 0 \quad 0 \quad 0 \quad C\beta_0 \quad S\beta_0]^T, 0 < \beta_0$, is refracted at the first boundary surface, $\bar{r}_1$. (6) Find unit normal vectors $\bar{n}_2$, D_2, E_2, λ_2, $C\theta_2$, N_2, the value of s_2 for the active unit normal vector, and $\bar{\ell}_2$ when ray $\bar{R}_1$ is refracted at the second boundary surface, $\bar{r}_2$. (7) Determine the ray displacement D.

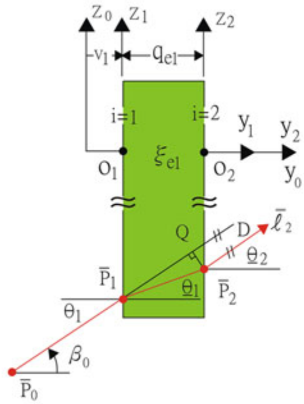

Fig. 2.14 Assigned coordinate frames $(xyz)_1$ and $(xyz)_2$ for rectangular optical flat

Solution

(1) The assigned coordinate frames $(xyz)_1$ and $(xyz)_2$ are shown in Fig. 2.14 with their origins, o_1 and o_2, located at any convenient in-plane points on boundary surfaces $\bar{r}_1$ and $\bar{r}_2$, respectively. Note that the y_1 and y_2 axes are both aligned with the y_0 axis of the world coordinate frame $(xyz)_0$.

(2) $^1\bar{n}_1 = s_1[0 \quad -1 \quad 0 \quad 0]^T$,
$^2\bar{n}_2 = s_2[0 \quad -1 \quad 0 \quad 0]^T$.

(3) If o_1 lies on the y_0 axis, then

$$^0\bar{A}_1 = \mathrm{tran}(0, v_1, 0) = \begin{bmatrix} 1 & 0 & 0 & 0 \\ 0 & 1 & 0 & v_1 \\ 0 & 0 & 1 & 0 \\ 0 & 0 & 0 & 1 \end{bmatrix},$$

$$\bar{X}_1 = [J_{1x} \quad J_{1y} \quad J_{1z} \quad e_1 \quad \xi_0 \quad \xi_1]^T = [0 \quad 1 \quad 0 \quad -v_1 \quad 1 \quad \xi_{e1}]^T.$$

(4) If o_2 lies on the y_0 axis, then

$$^0\bar{A}_2 = \mathrm{tran}(0, v_1 + q_{e1}, 0) = \begin{bmatrix} 1 & 0 & 0 & 0 \\ 0 & 1 & 0 & v_1 + q_{e1} \\ 0 & 0 & 1 & 0 \\ 0 & 0 & 0 & 1 \end{bmatrix},$$

$$\bar{X}_2 = [J_{2x} \quad J_{2y} \quad J_{2z} \quad e_2 \quad \xi_1 \quad \xi_2]^T = [0 \quad 1 \quad 0 \quad -(v_1 + q_{e1}) \quad 1 \quad 1]^T.$$

(5) $\bar{n}_1 = {}^0\bar{A}_1{}^1\bar{n}_1 = s_1[0 \quad -1 \quad 0 \quad 0]^T$,
$D_1 = -v_1$,
$E_1 = C\beta_0$,
$\lambda_1 = v_1/C\beta_0$,
$\bar{P}_1 = [0 \quad v_1 \quad v_1 S\beta_0/C\beta_0 \quad 1]^T$,
$\beta_1 = v_1 S\beta_0/C\beta_0$,
$\alpha_1 = \mathrm{atan2}(0, v_1 S\beta_0/C\beta_0) = 0°$,
$C\theta_1 = C\beta_0$.
$N_1 = \xi_0/\xi_1 = 1/\xi_{e1}$,
The active unit normal vector of $\bar{r}_1$ is $\bar{n}_1 = [0 \quad -1 \quad 0 \quad 0]^T$, yielding $s_1 = 1$,
$\bar{\ell}_1 = \left[0 \quad \sqrt{1 - N_1^2 + (N_1 C\beta_0)^2} \quad N_1 S\beta_0 \quad 0\right]^T$.

(6) $\bar{n}_2 = {}^0\bar{A}_2{}^2\bar{n}_2 = s_2[0 \quad -1 \quad 0 \quad 0]^T$,
$D_2 = -q_{e1}$,
$E_2 = \sqrt{1 - N_1^2 + (N_1 C\beta_0)^2}$,
$\lambda_2 = q_{e1}/\sqrt{1 - N_1^2 + (N_1 C\beta_0)^2}$,
$C\theta_2 = \sqrt{1 - N_1^2 + (N_1 C\beta_0)^2}$.
$N_2 = \xi_1/\xi_2 = \xi_{e1} = 1/N_1$,
The active unit normal vector of $\bar{r}_2$ is $\bar{n}_2 = [0 \quad -1 \quad 0 \quad 0]^T$, yielding $s_2 = 1$,
$\bar{\ell}_2 = [0 \quad C\beta_0 \quad S\beta_0 \quad 0]^T$.
It is thus proven that the exit ray $\bar{R}_2$ is parallel to $\bar{R}_0$.

(7) From Fig. 2.14, it follows that
$D = [q_{e1}\tan\beta_0 - (P_{2z} - P_{1z})]C\beta_0 = q_{e1}S\beta_0 - \frac{q_{e1}S\beta_0 C\beta_0}{\sqrt{1-N_1^2+(N_1C\beta_0)^2}}$.
After expansion of $S(\theta_1 - \underline{\theta}_1)$ and substitution of $\underline{\theta}_1$ from $S\theta_1 = N_1 S\underline{\theta}_1$ and $\theta_1 = \beta_0$, D can be reformulated as

$$D = q_{e1}S\beta_0\left(1 - \frac{C\beta_0}{\sqrt{N_1^2 - (S\beta_0)^2}}\right) = q_{e1}S\beta_0 - \frac{q_{e1}S\beta_0 C\beta_0}{\sqrt{1 - N_1^2 + (N_1 C\beta_0)^2}}.$$

Example 2.4 Consider the triangular prism shown in Fig. 2.15 with vertex angle η_{e1} and refractive index $\xi_{e1} = 1.5$. (1) Assign boundary coordinate frames $(xyz)_1$ and $(xyz)_2$ to the two flat boundary surfaces, $\bar{r}_1$ and $\bar{r}_2$. (2) Determine the pose matrices ${}^0\bar{A}_1$ and ${}^0\bar{A}_2$. (3) Find the unit normal vectors $\bar{n}_1$, D_1, E_1, λ_1, β_1, α_1, $C\theta_1$, N_1, the value of s_1 for the active unit normal vector, and $\bar{\ell}_1$ when ray $\bar{R}_0 =$

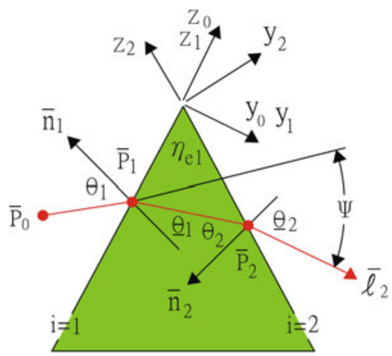

Fig. 2.15 Assigned coordinate frames $(xyz)_1$ and $(xyz)_2$ for triangular prism

$[0 \quad P_{0y} \quad P_{0z} \quad 0 \quad C\beta_0 \quad S\beta_0]^T$ ($P_{0y} < 0$, $P_{0z} < 0, P_{0z} - P_{0y}S\beta_0/C\beta_0 < 0$, and $0 < \beta_0$) is refracted at the first boundary surface, $\bar{r}_1$. (4) Find the unit normal vectors $\bar{n}_2$, D_2, E_2, λ_2, β_2, α_2, $C\theta_2$, the value of s_2 for the active unit normal vector when ray $\bar{R}_1$ is refracted at the second boundary surface, $\bar{r}_2$. (5) Determine the ray deviation angle ψ $(0 \le \psi \le 180°)$ in terms of θ_1, η_{e1} and N_1.

Solution

(1) The assigned coordinate frames $(xyz)_1$ and $(xyz)_2$ are shown in Fig. 2.15 with their origins both coinciding with the origin of $(xyz)_0$.

(2) $${}^0\bar{A}_1 = \bar{I}_{4\times4} = \begin{bmatrix} 1 & 0 & 0 & 0 \\ 0 & 1 & 0 & 0 \\ 0 & 0 & 1 & 0 \\ 0 & 0 & 0 & 1 \end{bmatrix},$$

$${}^0\bar{A}_2 = \mathrm{rot}(\bar{x}, \eta_{e1}) = \begin{bmatrix} 1 & 0 & 0 & 0 \\ 0 & C\eta_{e1} & -S\eta_{e1} & 0 \\ 0 & S\eta_{e1} & C\eta_{e1} & 0 \\ 0 & 0 & 0 & 1 \end{bmatrix}.$$

(3) $\bar{n}_1 = s_1[0 \quad -1 \quad 0 \quad 0]^T$ with $s_1 = \pm 1$
$D_1 = P_{0y}$,
$E_1 = C\beta_0$,
$\lambda_1 = -P_{0y}/C\beta_0$,
$\bar{P}_1 = [0 \quad 0 \quad P_{0z} - P_{0y}S\beta_0/C\beta_0 \quad 1]^T$,
$\beta_1 = -(P_{0z} - P_{0y}S\beta_0/C\beta_0)$,
$\alpha_1 = \mathrm{atan2}(0, P_{0z} - P_{0y}S\beta_0/C\beta_0) = 180°$,
$C\theta_1 = C\beta_0$.
$N_1 = \xi_0/\xi_1 = 1/\xi_{e1}$,
The active unit normal vector of $\bar{r}_1$ is $\bar{n}_1 = [0 \quad -1 \quad 0 \quad 0]^T$, leading to $s_1 = 1$,

$$\bar{\ell}_1 = \left[0 \quad \sqrt{1 - N_1^2 + (N_1 C\beta_0)^2} \quad N_1 S\beta_0 \quad 0\right]^T.$$

(4) $\bar{n}_2 = s_2[0 \quad -C\eta_{e1} \quad -S\eta_{e1} \quad 0]^T$ with $s_2 = \pm 1$,

$$D_2 = S\eta_{e1}\left(P_{0z} - P_{0y}S\beta_0/C\beta_0\right),$$

$$E_2 = C\eta_{e1}\sqrt{1 - N_1^2 + (N_1C\beta_0)^2} + N_1 S\eta_{e1} S\beta_0,$$

$$\lambda_2 = \frac{-S\eta_{e1}\left(P_{0z} - P_{0y}S\beta_0/C\beta_0\right)}{C\eta_{e1}\sqrt{1 - N_1^2 + (N_1C\beta_0)^2} + N_1 S\eta_{e1} S\beta_0},$$

$$C\theta_2 = C\eta_{e1}\sqrt{1 - N_1^2 + (N_1C\beta_0)^2} + N_1 S\beta_0 S\eta_{e1}.$$

The active unit normal vector of $\bar{r}_2$ is $\bar{n}_2 = [0 \quad -C\eta_{e1} \quad -S\eta_{e1} \quad 0]^T$, leading to $s_2 = 1$.

(5) It is possible to obtain $\bar{\ell}_2$ from Eq. (2.46) so as to determine ψ as $C\psi = \bar{\ell}_0 \cdot \bar{\ell}_2$. Alternatively, Snell's law can be applied successively at the two boundary surfaces to give $S\theta_1 = N_1 S\underline{\theta}_1$ and $S\theta_2 = N_2 S\underline{\theta}_2 = S\underline{\theta}_2/N_1$, respectively. Applying $\theta_2 = \eta_{e1} - \underline{\theta}_1$, it follows that

$$\begin{aligned}\psi &= \theta_1 - \underline{\theta}_1 + \underline{\theta}_2 - \theta_2 = \theta_1 + \underline{\theta}_2 - \eta_{e1} \\ &= \theta_1 - \eta_{e1} + \sin^{-1}\left(S\eta_{e1}\sqrt{\xi_{e1}^2 - (S\theta_1)^2} - C\eta_{e1} S\theta_1\right).\end{aligned}$$

In general, the refraction index is higher for short wavelengths (blue light) than for long wavelengths (red light). Therefore, the deviation angle ψ will be greater for blue light than for red.

The minimum deviation angle $\psi_{\min i}$ is found to occur when $\theta_1 = \underline{\theta}_2$ by setting $\partial\psi/\partial\theta_1 = 0$. Under this condition, the refractive index of the prism is given as

$$\xi_{e1} = \frac{S((\psi_{\min i} + \eta_{e1})/2)}{S(\eta_{e1}/2)}.$$

It is noted that this formulation provides a precise and convenient approach for measuring the refractive index ξ_{e1} since the minimum deviation angle $\psi_{\min i}$ can be readily determined using a spectrometer.

Example 2.5 The following example derives the raytracing equations for a meridional ray $\bar{R}_{i-1}$ incident on a flat boundary surface $\bar{r}_i$ in an axis-symmetrical system. As shown in Fig. 2.16, the flat boundary surface $\bar{r}_i$ is located at $y_0 = v_i$ and is oriented perpendicularly to the optical axis. The meridional ray $\bar{R}_{i-1}$ originates at point $\bar{P}_{i-1} = [0 \quad P_{i-1y} \quad P_{i-1z} \quad 1]^T$, travels along $\bar{\ell}_{i-1} = [0 \quad \ell_{i-1y} \quad \ell_{i-1z} \quad 0]^T$ ($\ell_{i-1y}^2 + \ell_{i-1z}^2 = 1$ with $0 < \ell_{i-1y}$ and $\ell_{i-1z} < 0$), and is then reflected or refracted at $\bar{r}_i$ with a unit normal vector $\bar{n}_i = s_i[0 \quad -1 \quad 0 \quad 0]^T$ ($s_i = \pm 1$). The incidence point $\bar{P}_i$ at which the ray strikes $\bar{r}_i$ is given by

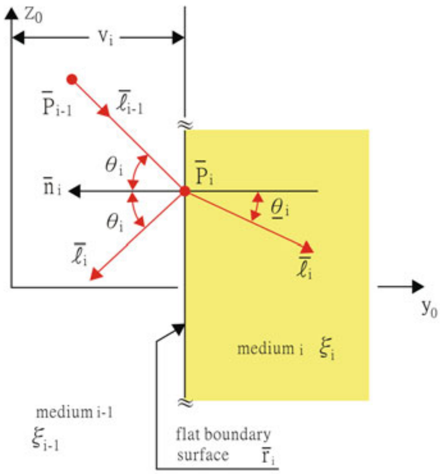

Fig. 2.16 Tracing meridional ray at flat boundary surface of axis-symmetrical system

$$\bar{P}_i = \begin{bmatrix} 0 \\ P_{iy} \\ P_{iz} \\ 1 \end{bmatrix} = \bar{P}_{i-1} + \lambda_i \bar{\ell}_{i-1} = \begin{bmatrix} 0 \\ P_{i-1y} + \lambda_i \ell_{i-1y} \\ P_{i-1z} + \lambda_i \ell_{i-1z} \\ 1 \end{bmatrix},$$

where the parameter λ_i is obtained by setting $P_{i-1y} + \lambda_i \ell_{i-1y} = v_i$, yielding

$$\lambda_i = \frac{v_i - P_{i-1y}}{\ell_{i-1y}}.$$

The incidence angle θ_i is given by $C\theta_i = \left|\bar{\ell}_{i-1} \cdot \bar{n}_i\right| = (-\bar{\ell}_{i-1}) \cdot \bar{n}_i = \ell_{i-1y}$, where the active unit normal vector has the form $\bar{n}_i = [0 \quad -1 \quad 0 \quad 0]^T$. The reflected unit directional vector $\bar{\ell}_i$ is then obtained by rotating the active unit normal vector $\bar{n}_i$ about the x_0 axis through an angle θ_i. Imposing $\ell^2_{i-1y} + \ell^2_{i-1z} = 1$, the reflected unit directional vector $\bar{\ell}_i$ is thus obtained as

$$\bar{\ell}_i = \begin{bmatrix} 0 \\ \ell_{iy} \\ \ell_{iz} \\ 0 \end{bmatrix} = \mathrm{rot}(\bar{x}, \theta_i)\, \bar{n}_i = \begin{bmatrix} 0 \\ -C\theta_i \\ -S\theta_i \\ 0 \end{bmatrix} = \begin{bmatrix} 0 \\ -\ell_{i-1y} \\ -\sqrt{1 - \ell^2_{i-1y}} \\ 0 \end{bmatrix}.$$

The refracted unit directional vector $\bar{\ell}_i$ can be obtained by rotating the active unit normal vector $\bar{n}_i$ about the x_0 axis through an angle $\pi - \underline{\theta}_i$, i.e.,

$$\bar{\ell}_i = \begin{bmatrix} 0 \\ \ell_{iy} \\ \ell_{iz} \\ 0 \end{bmatrix} = \text{rot}(\bar{x}, \pi - \underline{\theta}_i)\bar{n}_i = \begin{bmatrix} 0 \\ C\underline{\theta}_i \\ -S\underline{\theta}_i \\ 0 \end{bmatrix}.$$

The refraction angle $\underline{\theta}_i$ must satisfy Snell's law, i.e., $S\underline{\theta}_i = (\xi_{i-1}/\xi_i)S\theta_i = N_i S\theta_i$. Consequently, the refracted unit directional vector $\bar{\ell}_i$ can be formulated as

$$\bar{\ell}_i = \begin{bmatrix} 0 \\ \ell_{iy} \\ \ell_{iz} \\ 0 \end{bmatrix} = \begin{bmatrix} 0 \\ \sqrt{1 - N_i^2 + (N_i \ell_{i-1y})^2} \\ -N_i \sqrt{1 - \ell_{i-1y}^2} \\ 0 \end{bmatrix}.$$

It is noted that when the source ray $\bar{R}_{i-1}$ travels in the upward direction (i.e., $0 < \ell_{i-1z}$), the unit directional vectors of the reflected and refracted rays are computed as $\bar{\ell}_i = \text{rot}(-\bar{x}, \theta_i)\bar{n}_i$ and $\bar{\ell}_i = \text{rot}(-\bar{x}, \pi - \underline{\theta}_i)\bar{n}_i$, respectively, where $\bar{n}_i = \begin{bmatrix} 0 & -1 & 0 & 0 \end{bmatrix}^T$ is the active unit normal vector.

2.4 General Aspherical Boundary Surfaces

Most optical systems comprise flat or spherical boundary surfaces since such surfaces are easily manufactured with low cost. However, certain systems also contain aspherical boundary surfaces. Accordingly, this section extends the raytracing methodology described above to the case of aspherical boundary surfaces ([10, 35–37], p. 312 of [34]). In practice, the ability to trace rays at aspherical boundary surfaces is highly important since even though such surfaces are difficult and expensive to manufacture, there are cases where elements with aspherical boundary surfaces have significant advantages over those with spherical boundary surfaces.

2.4.1 Aspherical Boundary Surface and Associated Unit Normal Vector

While in principle an aspherical surface can take a wide variety of forms, any aspherical boundary surface can be designed with a generating curve ${}^i\bar{q}_i$ of the form

$${}^i\bar{q}_i = \begin{bmatrix} 0 \\ y_i(\beta_i) \\ z_i(\beta_i) \\ 1 \end{bmatrix} (0 \le z_i(\beta_i)), \tag{2.49}$$

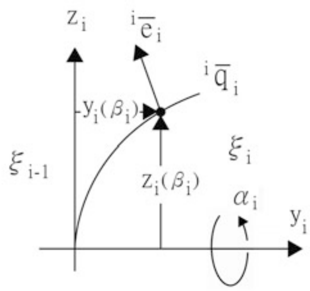

Fig. 2.17 Generating curve for aspherical boundary surface

where the optical axis is presumed to lie in the y_i axis direction and $y_i(\beta_i)$ is the sag (i.e., the y_i component of the displacement from the vertex at distance $z_i(\beta_i)$ from the optical axis) (Fig. 2.17, in which $(xyz)_i$ is the boundary coordinate frame). The two unit normal vectors of the generating curve have the form

$$
{}^i\bar{\eta}_i = \begin{bmatrix} \eta_{ix} \\ \eta_{iy} \\ \eta_{iz} \\ 0 \end{bmatrix} = \frac{s_i}{\sqrt{[d(y_i(\beta_i))/d\beta_i]^2 + [d(z_i(\beta_i))/d\beta_i]^2}} \begin{bmatrix} 0 \\ -d(z_i(\beta_i))/d\beta_i \\ d(y_i(\beta_i))/d\beta_i \\ 0 \end{bmatrix}
$$
$$
= \frac{s_i}{\sqrt{y_i'^2 + z_i'^2}} \begin{bmatrix} 0 \\ -z_i' \\ y_i' \\ 0 \end{bmatrix}, \tag{2.50}
$$

where s_i is again set to either +1 or −1 to indicate the existence of two possible unit normal vectors with directions opposite to one another. The aspherical boundary surface ${}^i\bar{r}_i$ and its two unit normal vectors ${}^i\bar{n}_i$ can be obtained by rotating ${}^i\bar{q}_i$ and ${}^i\bar{\eta}_i$, respectively, about the y_i axis through an angle α_i ($0 \le \alpha_i < 2\pi$), i.e.,

$$
{}^i\bar{r}_i = \begin{bmatrix} x_i \\ y_i \\ z_i \\ 1 \end{bmatrix} = \text{rot}(\bar{y}, \alpha_i)\,{}^i\bar{q}_i = \begin{bmatrix} C\alpha_i & 0 & S\alpha_i & 0 \\ 0 & 1 & 0 & 0 \\ -S\alpha_i & 0 & C\alpha_i & 0 \\ 0 & 0 & 0 & 1 \end{bmatrix} \begin{bmatrix} 0 \\ y_i(\beta_i) \\ z_i(\beta_i) \\ 1 \end{bmatrix}
$$
$$
= \begin{bmatrix} z_i(\beta_i)S\alpha_i \\ y_i(\beta_i) \\ z_i(\beta_i)C\alpha_i \\ 1 \end{bmatrix}, \tag{2.51}
$$

$$
\begin{aligned}
{}^{i}\bar{n}_i = \mathrm{rot}(\bar{y}, \alpha_i)\,{}^{i}\bar{\eta}_i &= \begin{bmatrix} C\alpha_i & 0 & S\alpha_i & 0 \\ 0 & 1 & 0 & 0 \\ -S\alpha_i & 0 & C\alpha_i & 0 \\ 0 & 0 & 0 & 1 \end{bmatrix} \begin{bmatrix} \eta_{ix} \\ \eta_{iy} \\ \eta_{iz} \\ 0 \end{bmatrix} \\
&= \frac{s_i}{\sqrt{y_i'^2 + z_i'^2}} \begin{bmatrix} y_i' S\alpha_i \\ -z_i' \\ y_i' C\alpha_i \\ 0 \end{bmatrix}.
\end{aligned}
\tag{2.52}
$$

Equations (2.51) and (2.52) give ${}^{i}\bar{r}_i$ and ${}^{i}\bar{n}_i$ with respect to the coordinate frame $(xyz)_i$. However, many derivations in this book are referred to the world coordinate frame $(xyz)_o$. Consequently, the pose matrix ${}^{0}\bar{A}_i$ of $(xyz)_i$ with respect to $(xyz)_0$ given in Eq. (2.9) is required. The unit normal vectors of the aspherical surface relative to the world coordinate frame $(xyz)_0$ can then be obtained from the following transformation:

$$
\begin{aligned}
\bar{n}_i = \begin{bmatrix} n_{ix} \\ n_{iy} \\ n_{iz} \\ 0 \end{bmatrix} = {}^{0}\bar{A}_i\,{}^{i}\bar{n}_i &= \frac{s_i}{\sqrt{y_i'^2 + z_i'^2}} \begin{bmatrix} I_{ix} & J_{ix} & K_{ix} & t_{ix} \\ I_{iy} & J_{iy} & K_{iy} & t_{iy} \\ I_{iz} & J_{iz} & K_{iz} & t_{iz} \\ 0 & 0 & 0 & 1 \end{bmatrix} \begin{bmatrix} y_i' S\alpha_i \\ -z_i' \\ y_i' C\alpha_i \\ 0 \end{bmatrix}. \\
&= \frac{s_i}{\sqrt{y_i'^2 + z_i'^2}} \begin{bmatrix} I_{ix} y_i' S\alpha_i - J_{ix} z_i' + K_{ix} y_i' C\alpha_i \\ I_{iy} y_i' S\alpha_i - J_{iy} z_i' + K_{iy} y_i' C\alpha_i \\ I_{iz} y_i' S\alpha_i - J_{iz} z_i' + K_{iz} y_i' C\alpha_i \\ 0 \end{bmatrix}.
\end{aligned}
\tag{2.53}
$$

2.4.2 Incidence Point

Figure 2.18 shows a typical ray path at an aspherical boundary surface. As shown, the ray originates from point $\bar{P}_{i-1}$ on the previous boundary surface $\bar{r}_{i-1}$ and travels along the unit directional vector $\bar{\ell}_{i-1}$ until it is reflected or refracted at current boundary surface $\bar{r}_i$. Any intermediate point $\bar{P}'_{i-1}$ lying along this ray as it travels from $\bar{P}_{i-1}$ toward $\bar{r}_i$ is given by $\bar{P}'_{i-1} = \bar{P}_{i-1} + \lambda \bar{\ell}_{i-1}$. Let λ_i represent the geometrical path distance from point $\bar{P}_{i-1}$ to the incidence point $\bar{P}_i$ on boundary surface $\bar{r}_i$. The incidence point $\bar{P}_i$ on the boundary surface is given as $\bar{P}_i = \bar{P}_{i-1} + \lambda_i \bar{\ell}_{i-1}$. To solve for λ_i, α_i and β_i, it is necessary to transform $\bar{P}_i$ to coordinate frame $(xyz)_i$ and then equate the result with the boundary surface ${}^{i}\bar{r}_i$ (Eq. (2.51)), i.e.,

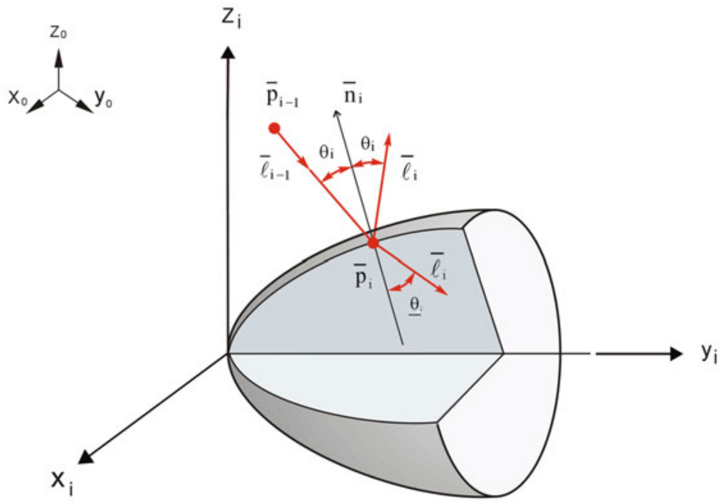

Fig. 2.18 Raytracing at aspherical boundary surface

$$
{}^{i}\bar{P}_i = {}^{i}\bar{A}_0\bar{P}_i = ({}^{0}\bar{A}_i)^{-1}\bar{P}_i = \begin{bmatrix} \sigma_i \\ \rho_i \\ \tau_i \\ 1 \end{bmatrix} = {}^{i}\bar{r}_i = \begin{bmatrix} z_i(\beta_i)S\alpha_i \\ y_i(\beta_i) \\ z_i(\beta_i)C\alpha_i \\ 1 \end{bmatrix}, \tag{2.54}
$$

where σ_i, ρ_i and τ_i are defined in Eqs. (2.13), (2.14) and (2.15), respectively. The value of parameter α_i at incidence point $\bar{P}_i$ can then be obtained from the first and third components of Eq. (2.54) using the following function:

$$
\begin{cases} \alpha_i = \operatorname{atan2}(\sigma_i, \tau_i) & \text{when } z_i(\beta_i) > 0 \\ \alpha_i = \text{any value} & \text{when } z_i(\beta_i) = 0. \end{cases} \tag{2.55}
$$

Meanwhile, the values of parameters λ_i and β_i at incidence point $\bar{P}_i$ can be determined from the following two independent equations:

$$
z_i(\beta_i)^2 = \sigma_i^2 + \tau_i^2, \tag{2.56}
$$

$$
y_i(\beta_i) = \rho_i. \tag{2.57}
$$

The difficulty in tracing a skew-ray at a general aspherical surface lies in determining λ_i from Eqs. (2.56) and (2.57) since the solution cannot usually be determined directly. In other words, some form of numerical method is required (e.g., p. 314 of [34]). However, by adopting a similar procedure to that described in Sect. 2.2, the expressions given in Eqs. (2.26) and (2.29) are still valid for the reflected and refracted unit directional vectors $\bar{\ell}_i$, respectively.

The boundary variable vector $\bar{X}_i$ of the aspherical boundary surface is given as

$$\bar{X}_i = \begin{bmatrix} t_{ix} & t_{iy} & t_{iz} & \omega_{ix} & \omega_{iy} & \omega_{iz} & \xi_{i-1} & \xi_i & \overline{coef_i} \end{bmatrix}^T, \tag{2.58}$$

where $t_{ix}, t_{iy}, t_{iz}, \omega_{ix}, \omega_{iy}$ and ω_{iz} are the six pose variables of the boundary surface; ξ_{i-1} and ξ_i are the refractive indices of media i − 1 and i, respectively; and $\overline{coef_i}$ contains the independent coefficients of $y_i(\beta_i)$ and $z_i(\beta_i)$.

Example 2.6 For an ellipsoidal boundary surface (Fig. 2.19), the generating curve is given as

$$\begin{aligned} {}^i\bar{q}_i &= [0 \quad y_i(\beta_i) \quad z_i(\beta_i) \quad 1]^T \\ &= [0 \quad a_i S\beta_i \quad b_i C\beta_i \quad 1]^T (0 < a_i, 0 < b_i, -\frac{\pi}{2} \le \beta_i \le \frac{\pi}{2}), \end{aligned}$$

where the geometrical path length λ_i, β_i, and boundary variable vector $\bar{X}_i$ are given respectively as

$$\begin{aligned} \lambda_i &= \frac{-D_i \pm \sqrt{D_i^2 - H_i E_i}}{H_i}, \\ \beta_i &= \operatorname{atan2}\left(\frac{\rho_i}{a_i}, \frac{\sqrt{\sigma_i^2 + \tau_i^2}}{b_i}\right), \\ \bar{X}_i &= [t_{ix} \quad t_{iy} \quad t_{iz} \quad \omega_{ix} \quad \omega_{iy} \quad \omega_{iz} \quad \xi_{i-1} \quad \xi_i \quad a_i \quad b_i]^T, \end{aligned}$$

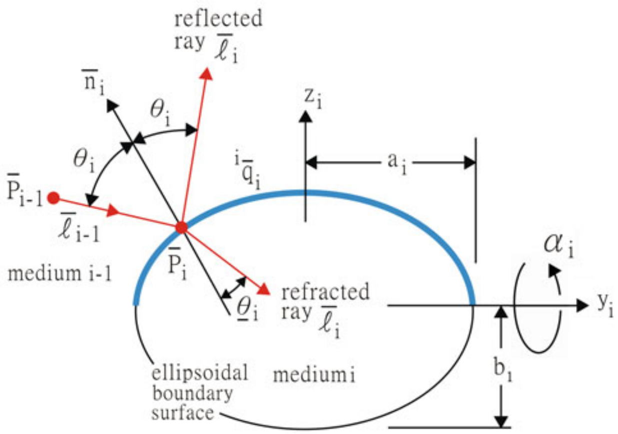

Fig. 2.19 Raytracing at ellipsoidal boundary surface

in which

$$\begin{aligned}
H_i &= 2\left(\frac{1}{a_i^2}-\frac{1}{b_i^2}\right)\left(J_{ix}J_{iy}\ell_{i-1x}\ell_{i-1y}+J_{ix}J_{iz}\ell_{i-1x}\ell_{i-1z}+J_{iy}J_{iz}\ell_{i-1y}\ell_{i-1z}\right)\\
&\quad+\frac{1}{b_i^2}+\left(\frac{1}{a_i^2}-\frac{1}{b_i^2}\right)\left(J_{ix}^2\ell_{i-1x}^2+J_{iy}^2\ell_{i-1y}^2+J_{iz}^2\ell_{i-1z}^2\right),\\
D_i &= \left(\frac{1}{b_i^2}-\frac{J_{ix}^2}{b_i^2}+\frac{J_{ix}^2}{a_i^2}\right)P_{i-1x}\ell_{i-1x}+\left(\frac{1}{b_i^2}-\frac{J_{iy}^2}{b_i^2}+\frac{J_{iy}^2}{a_i^2}\right)P_{i-1y}\ell_{i-1y}+\left(\frac{1}{b_i^2}-\frac{J_{iz}^2}{b_i^2}+\frac{J_{iz}^2}{a_i^2}\right)P_{i-1z}\ell_{i-1z}\\
&\quad+\left(\frac{1}{a_i^2}-\frac{1}{b_i^2}\right)\left[J_{ix}J_{iy}\left(P_{i-1x}\ell_{i-1y}+\ell_{i-1x}P_{i-1y}\right)+J_{ix}J_{iz}\left(P_{i-1x}\ell_{i-1z}+\ell_{i-1x}P_{i-1z}\right)\right.\\
&\quad\left.+J_{iy}J_{iz}\left(P_{i-1y}\ell_{i-1z}+\ell_{i-1y}P_{i-1z}\right)\right]-\frac{\left(t_{ix}\ell_{i-1x}+t_{iy}\ell_{i-1y}+t_{iz}\ell_{i-1z}\right)}{b_i^2}\\
&\quad+\left(\frac{1}{b_i^2}-\frac{1}{a_i^2}\right)\left(J_{ix}t_{ix}+J_{iy}t_{iy}+J_{iz}t_{iz}\right)\left(J_{ix}\ell_{i-1x}+J_{iy}\ell_{i-1y}+J_{iz}\ell_{i-1z}\right),\\
E_i &= \left(\frac{1}{b_i^2}-\frac{J_{ix}^2}{b_i^2}+\frac{J_{ix}^2}{a_i^2}\right)P_{i-1x}^2+\left(\frac{1}{b_i^2}-\frac{J_{iy}^2}{b_i^2}+\frac{J_{iy}^2}{a_i^2}\right)P_{i-1y}^2+\left(\frac{1}{b_i^2}-\frac{J_{iz}^2}{b_i^2}+\frac{J_{iz}^2}{a_i^2}\right)P_{i-1z}^2\\
&\quad+\frac{t_{ix}^2}{b_i^2}+\frac{t_{iy}^2}{a_i^2}+\frac{t_{iz}^2}{b_i^2}-\frac{2}{b_i^2}\left(t_{ix}P_{i-1x}+t_{iy}P_{i-1y}+t_{iz}P_{i-1z}\right)-1\\
&\quad+2\left(\frac{1}{a_i^2}-\frac{1}{b_i^2}\right)\left(J_{ix}J_{iy}P_{i-1x}P_{i-1y}+J_{ix}J_{iz}P_{i-1x}P_{i-1z}+J_{iy}J_{iz}P_{i-1y}P_{i-1z}\right)\\
&\quad-2\left(\frac{1}{a_i^2}-\frac{1}{b_i^2}\right)\left(t_{ix}J_{ix}+t_{iy}J_{iy}+t_{iz}J_{iz}\right)\left(J_{ix}P_{i-1x}+J_{iy}P_{i-1y}+J_{iz}P_{i-1z}\right).
\end{aligned}$$

$\beta_i = \pm\pi/2$ are two pseudo-singular points on the ellipsoidal boundary surface. The cross product $\partial^i\bar{r}_i/\partial\beta_i \times \partial^i\bar{r}_i/\partial\alpha_i$ cannot be obtained at these two points, and thus some difficulties occur in computing the point spread function and modulation transfer function.

Example 2.7 The boundary variable vector $\bar{X}_i$ of a paraboloidal boundary surface defined by generating curve (see Fig. 2.20)

$$^i\bar{q}_i = \begin{bmatrix}0 & y_i(\beta_i) & z_i(\beta_i) & 1\end{bmatrix}^T = \begin{bmatrix}0 & a_i\beta_i^2 & \beta_i & 1\end{bmatrix}^T (0 \le \beta_i, 0 < a_i)$$

is given by

$$\bar{X}_i = \begin{bmatrix}t_{ix} & t_{iy} & t_{iz} & \omega_{ix} & \omega_{iy} & \omega_{iz} & \xi_{i-1} & \xi_i & a_i\end{bmatrix}^T.$$

Its geometrical path length λ_i is given as follows:

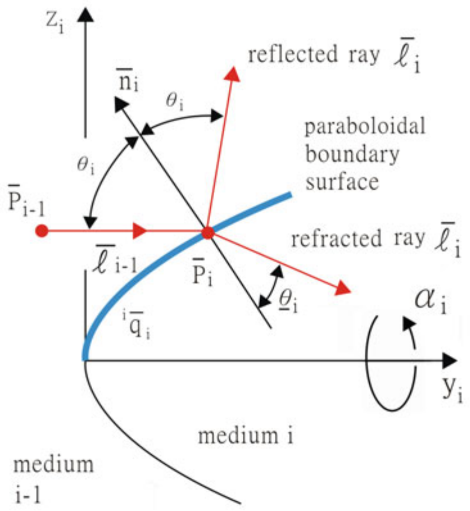

Fig. 2.20 Raytracing at paraboloidal boundary surface

(a) If $J_{ix}\ell_{i-1x} + J_{iy}\ell_{i-1y} + J_{iz}\ell_{i-1z} \neq \pm 1$, then

$$\lambda_i = \frac{-D_i \pm \sqrt{D_i^2 - H_i E_i}}{H_i},$$

where

$$\begin{aligned}
H_i &= 1 - \left(J_{ix}\ell_{i-1x} + J_{iy}\ell_{i-1y} + J_{iz}\ell_{i-1z}\right)^2,\\
D_i &= \left(1 - J_{ix}^2\right)P_{i-1x}\ell_{i-1x} + \left(1 - J_{iy}^2\right)P_{i-1y}\ell_{i-1y} + \left(1 - J_{iz}^2\right)P_{i-1z}\ell_{i-1z}\\
&\quad - \left(t_{ix}\ell_{i-1x} + t_{iy}\ell_{i-1y} + t_{iz}\ell_{i-1z}\right) - J_{ix}J_{iy}\left(P_{i-1x}\ell_{i-1y} + P_{i-1y}\ell_{i-1x}\right)\\
&\quad - J_{ix}J_{iz}\left(P_{i-1x}\ell_{i-1z} + P_{i-1z}\ell_{i-1x}\right) - J_{iy}J_{iz}\left(P_{i-1y}\ell_{i-1z} + P_{i-1z}\ell_{i-1y}\right)\\
&\quad + \left(J_{ix}t_{ix} + J_{iy}t_{iy} + J_{iz}t_{iz}\right)\left(J_{ix}\ell_{i-1x} + J_{iy}\ell_{i-1y} + J_{iz}\ell_{i-1z}\right)\\
&\quad - \left(J_{ix}\ell_{i-1x} + J_{iy}\ell_{i-1y} + J_{iz}\ell_{i-1z}\right)/(2a_i),\\
E_i &= \left(P_{i-1x}^2 + P_{i-1y}^2 + P_{i-1z}^2\right) + t_{ix}^2 + t_{iy}^2 + t_{iz}^2 - 2\left(t_{ix}P_{i-1x} + t_{iy}P_{i-1y} + t_{iz}P_{i-1z}\right)\\
&\quad + \left[J_{ix}\left(t_{ix} + P_{i-1x}\right) + J_{iy}\left(t_{iy} + P_{i-1y}\right) + J_{iz}\left(t_{iz} + P_{i-1z}\right)\right]^2\\
&\quad + \left[J_{ix}\left(t_{ix} - P_{i-1x}\right) + J_{iy}\left(t_{iy} - P_{i-1y}\right) + J_{iz}\left(t_{iz} - P_{i-1z}\right)\right]/a_i.
\end{aligned}$$

(b) If $J_{ix}\ell_{i-1x} + J_{iy}\ell_{i-1y} + J_{iz}\ell_{i-1z} = \pm 1$, then

$$\lambda_i = \frac{D_i}{H_i},$$

where

$$\begin{aligned} D_i &= J_{ix}(t_{ix} - P_{i-1x}) + J_{iy}(t_{iy} - P_{i-1y}) + J_{iz}(t_{iz} - P_{i-1z}) \\ &\quad + a_i\left[(t_{ix} - P_{i-1x})^2 + (t_{iy} - P_{i-1y})^2 + (t_{iz} - P_{i-1z})^2\right] \\ &\quad - a_i\left[J_{ix}(t_{ix} - P_{i-1x}) + J_{iy}(t_{iy} - P_{i-1y}) + J_{iz}(t_{iz} - P_{i-1z})\right]^2, \\ H_i &= J_{ix}\ell_{i-1x} + J_{iy}\ell_{i-1y} + J_{iz}\ell_{i-1z}, \end{aligned}$$

$\beta_i = 0$ is the only pseudo-singular point on the paraboloidal boundary surface.

Example 2.8 The geometrical path length λ_i of a hyperboloidal boundary surface defined by the generating curve (see Fig. 2.21)

$$\begin{aligned} {}^i\bar{q}_i &= [0 \quad y_i(\beta_i) \quad z_i(\beta_i) \quad 1]^T \\ &= [0 \quad a_i/C\beta_i \quad b_iS\beta_i/C\beta_i \quad 1]^T (0 \le \beta_i < \pi/2, 0 < a_i, 0 < b_i) \end{aligned}$$

is given by

$$\lambda_i = \frac{-D_i \pm \sqrt{D_i^2 - H_iE_i}}{H_i},$$

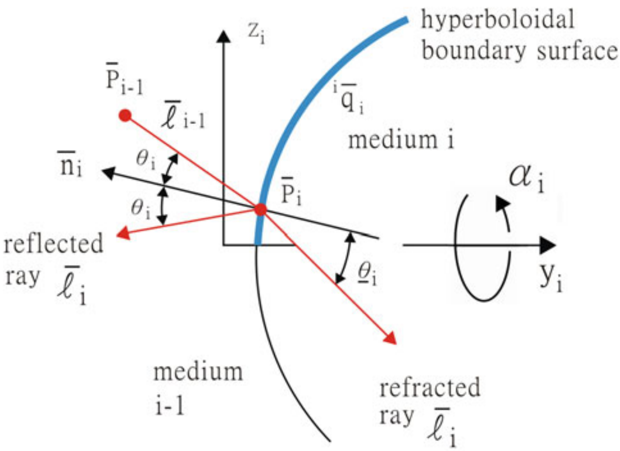

Fig. 2.21 Raytracing at hyperboloidal boundary surface

where

$$
\begin{aligned}
H_i = {} & \left(\frac{1}{b_i^2}-\frac{J_{ix}^2}{b_i^2}-\frac{J_{ix}^2}{a_i^2}\right)\ell_{i-1x}^2+\left(\frac{1}{b_i^2}-\frac{J_{iy}^2}{b_i^2}-\frac{J_{iy}^2}{a_i^2}\right)\ell_{i-1y}^2+\left(\frac{1}{b_i^2}-\frac{J_{iz}^2}{b_i^2}-\frac{J_{iz}^2}{a_i^2}\right)\ell_{i-1z}^2 \\
& -2\left(\frac{1}{a_i^2}+\frac{1}{b_i^2}\right)\left(J_{ix}J_{iy}\ell_{i-1x}\ell_{i-1y}+J_{ix}J_{iz}\ell_{i-1x}\ell_{i-1z}+J_{iy}J_{iz}\ell_{i-1y}\ell_{i-1z}\right), \\
D_i = {} & \left(\frac{1}{b_i^2}-\frac{J_{ix}^2}{b_i^2}-\frac{J_{ix}^2}{a_i^2}\right)P_{i-1x}\ell_{i-1x}+\left(\frac{1}{b_i^2}-\frac{J_{iy}^2}{b_i^2}-\frac{J_{iy}^2}{a_i^2}\right)P_{i-1y}\ell_{i-1y}+\left(\frac{1}{b_i^2}-\frac{J_{iz}^2}{b_i^2}-\frac{J_{iz}^2}{a_i^2}\right)P_{i-1z}\ell_{i-1z} \\
& -\left(\frac{1}{a_i^2}+\frac{1}{b_i^2}\right)\left[J_{ix}J_{iy}(P_{i-1x}\ell_{i-1y}+P_{i-1y}\ell_{i-1x})+J_{ix}J_{iz}(P_{i-1x}\ell_{i-1z}+P_{i-1z}\ell_{i-1x})\right. \\
& \left.+J_{iy}J_{iz}(P_{i-1y}\ell_{i-1z}+P_{i-1z}\ell_{i-1y})\right]-\left(\ell_{i-1x}t_{ix}+\ell_{i-1y}t_{iy}+\ell_{i-1z}t_{iz}\right)/b_i^2 \\
& +\left(\frac{1}{a_i^2}+\frac{1}{b_i^2}\right)\left(J_{ix}\ell_{i-1x}+J_{iy}\ell_{i-1y}+J_{iz}\ell_{i-1z}\right)\left(J_{ix}t_{ix}+J_{iy}t_{iy}+J_{iz}t_{iz}\right), \\
E_i = {} & \left(\frac{1}{b_i^2}-\frac{J_{ix}^2}{b_i^2}-\frac{J_{ix}^2}{a_i^2}\right)P_{i-1x}^2+\left(\frac{1}{b_i^2}-\frac{J_{iy}^2}{b_i^2}-\frac{J_{iy}^2}{a_i^2}\right)P_{i-1y}^2+\left(\frac{1}{b_i^2}-\frac{J_{iz}^2}{b_i^2}-\frac{J_{iz}^2}{a_i^2}\right)P_{i-1z}^2 \\
& -2\left(\frac{1}{a_i^2}+\frac{1}{b_i^2}\right)\left(J_{ix}J_{iy}P_{i-1x}P_{i-1y}+J_{ix}J_{iz}P_{i-1x}P_{i-1z}+J_{iy}J_{iz}P_{i-1y}P_{i-1z}\right) \\
& +2\left(\frac{1}{a_i^2}+\frac{1}{b_i^2}\right)(J_{ix}P_{i-1x}+J_{iy}P_{i-1y}+J_{iz}P_{i-1z})(J_{ix}t_{ix}+J_{iy}t_{iy}+J_{iz}t_{iz}) \\
& -2(P_{i-1x}t_{ix}+P_{i-1y}t_{iy}+P_{i-1z}t_{iz})/b_i^2+(t_{ix}^2+t_{iy}^2+t_{iz}^2)/a_i^2+1.
\end{aligned}
$$

Its boundary variable vector $\bar{X}_i$ is

$$\bar{X}_i = \begin{bmatrix} t_{ix} & t_{iy} & t_{iz} & \omega_{ix} & \omega_{iy} & \omega_{iz} & \xi_{i-1} & \xi_i & a_i & b_i \end{bmatrix}^T.$$

$\beta_i = 0$ is the only pseudo-singular point on the hyperboloidal boundary surface.

Example 2.9 The geometrical path length λ_i of a cylindrical boundary surface defined by the generating curve (see Fig. 2.22)

$${}^i\bar{q}_i = \begin{bmatrix} 0 & y_i(\beta_i) & z_i(\beta_i) & 1 \end{bmatrix}^T = \begin{bmatrix} 0 & \beta_i & R_i & 1 \end{bmatrix}^T \; (0 \le \beta_i,\ 0 < R_i)$$

is given by

$$\lambda_i = \frac{-D_i \pm \sqrt{D_i^2 - H_i E_i}}{H_i},$$

Fig. 2.22 Raytracing at cylindrical boundary surface

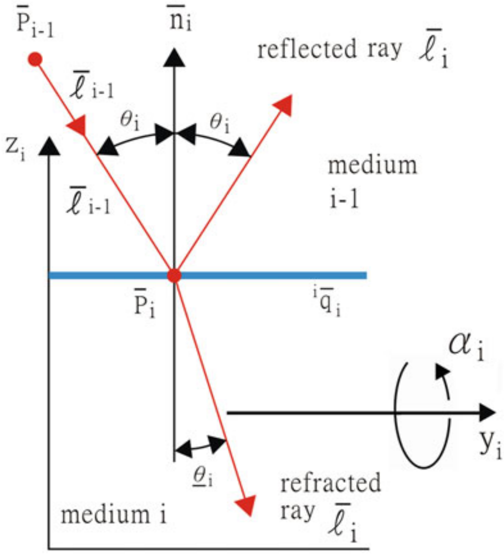

where

$$
\begin{aligned}
H_i &= 1 - (J_{ix}\ell_{i-1x} + J_{iy}\ell_{i-1y} + J_{iz}\ell_{i-1z})^2,\\
D_i &= (P_{i-1x} - t_{ix})\ell_{i-1x} + (P_{i-1y} - t_{iy})\ell_{i-1y} + (P_{i-1z} - t_{iz})\ell_{i-1z}\\
&\quad + [J_{ix}(t_{ix} - P_{i-1x}) + J_{iy}(t_{iy} - P_{i-1y}) + J_{iz}(t_{iz} - P_{i-1z})](J_{ix}\ell_{i-1x} + J_{iy}\ell_{i-1y} + J_{iz}\ell_{i-1z}),\\
E_i &= P^2_{i-1x} + P^2_{i-1y} + P^2_{i-1z} + t^2_{ix} + t^2_{iy} + t^2_{iz} - R^2_i - 2(t_{ix}P_{i-1x} + t_{iy}P_{i-1y} + t_{iz}P_{i-1z})\\
&\quad - \left[J_{ix}(t_{ix} - P_{i-1x}) + J_{iy}(t_{iy} - P_{i-1y}) + J_{iz}(t_{iz} - P_{i-1z})\right]^2.
\end{aligned}
$$

Its boundary variable vector $\bar{X}_i$ is

$$\bar{X}_i = [\, t_{ix} \quad t_{iy} \quad t_{iz} \quad \omega_{ix} \quad \omega_{iy} \quad \omega_{iz} \quad \xi_{i-1} \quad \xi_i \quad R_i \,]^T.$$

There are no pseudo-singular points on the cylindrical boundary surface.

2.5 The Unit Normal Vector of a Boundary Surface for Given Incoming and Outgoing Rays

In the sections above, Snell's law is used to determine the unit directional vectors $\bar{\ell}_i$ of the reflected and refracted rays for an incoming ray impinging on a boundary surface $\bar{r}_i$ between two different isotropic media. In this section, Snell's law is used to derive the active unit normal vector $\bar{n}_i$ at incidence point $\bar{P}_i$ on a boundary surface

$\bar{r}_i$ given the unit directional vectors of the incoming and outgoing rays (i.e., $\bar{\ell}_{i-1}$ and $\bar{\ell}_i$) [38–41]. Note that this problem has important applications in the design and fabrication of aspherical surfaces, since the surface normal vectors determine not only the optical performance of the surface, but also the cutting tool angles required to machine the surface.

2.5.1 Unit Normal Vector of Refractive Boundary Surface

As shown in Fig. 2.6, the design of a refractive surface requires a knowledge of the incidence angle θ_i and refraction angle $\underline{\theta}_i$ corresponding to the unit directional vectors of the incoming and outgoing rays (i.e., $\bar{\ell}_{i-1}$ and $\bar{\ell}_i$). In accordance with Snell's law (Eq. (2.22))

$$S\underline{\theta}_i = \frac{\xi_{i-1}}{\xi_i} S\theta_i = N_i S\theta_i,$$

the refraction phenomenon at the interface between two different isotropic media can be modeled as follows:

$$\bar{\ell}_{i-1} \cdot \bar{\ell}_i = C(\theta_i - \underline{\theta}_i) = C\theta_i C\underline{\theta}_i + S\theta_i S\underline{\theta}_i. \tag{2.59}$$

In geometrical optics, the incidence angle θ_i and refraction angle $\underline{\theta}_i$ lie in the domains of $0^\circ \le \theta_i \le 90^\circ$ and $0^\circ \le \underline{\theta}_i \le 90^\circ$. Since the trigonometric functions of θ_i and $\underline{\theta}_i$ are positive, the following four equations can be obtained from Eqs. (2.59) and (2.22):

$$S\theta_i = \frac{\sqrt{1 - (\bar{\ell}_{i-1} \cdot \bar{\ell}_i)^2}}{\sqrt{N_i^2 + 1 - 2N_i(\bar{\ell}_{i-1} \cdot \bar{\ell}_i)}}, \tag{2.60}$$

$$C\theta_i = \frac{\left|N_i - (\bar{\ell}_{i-1} \cdot \bar{\ell}_i)\right|}{\sqrt{N_i^2 + 1 - 2N_i(\bar{\ell}_{i-1} \cdot \bar{\ell}_i)}}, \tag{2.61}$$

$$S\underline{\theta}_i = \frac{N_i\sqrt{1 - (\bar{\ell}_{i-1} \cdot \bar{\ell}_i)^2}}{\sqrt{N_i^2 + 1 - 2N_i(\bar{\ell}_{i-1} \cdot \bar{\ell}_i)}}, \tag{2.62}$$

$$C\underline{\theta}_i = \frac{\left|1 - N_i(\bar{\ell}_{i-1} \cdot \bar{\ell}_i)\right|}{\sqrt{N_i^2 + 1 - 2N_i(\bar{\ell}_{i-1} \cdot \bar{\ell}_i)}}. \tag{2.63}$$

Referring to Fig. 2.6, to determine the active unit normal vector $\bar{n}_i$ at any incidence point $\bar{P}_i$ on a refractive surface $\bar{r}_i$, it is first necessary to compute the common unit normal $\bar{m}_i$ of the unit directional vectors $\bar{\ell}_{i-1}$ and $\bar{\ell}_i$ of the incoming and outgoing rays, respectively. Given the assumption $\theta_i \neq \underline{\theta}_i$ when $N_i \neq 1$, $\bar{m}_i$ can be obtained as

$$\bar{m}_i = \begin{bmatrix} m_{ix} & m_{iy} & m_{iz} & 0 \end{bmatrix}^T = \frac{\bar{\ell}_{i-1} \times \bar{\ell}_i}{S(\theta_i - \underline{\theta}_i)}. \tag{2.64}$$

To simplify the expression for the unit normal vector $\bar{n}_i$, it is useful to have the following equation, obtained by taking the post cross product of Eq. (2.64) by $S(\theta_i - \underline{\theta}_i)\bar{\ell}_{i-1}$, i.e.,

$$\begin{aligned} S(\theta_i - \underline{\theta}_i)\left(\bar{m}_i \times \bar{\ell}_{i-1}\right) &= (\bar{\ell}_{i-1} \times \bar{\ell}_i) \times \bar{\ell}_{i-1} = \bar{\ell}_i(\bar{\ell}_{i-1} \cdot \bar{\ell}_{i-1}) - \bar{\ell}_{i-1}(\bar{\ell}_i \cdot \bar{\ell}_{i-1}) \\ &= \bar{\ell}_i - \bar{\ell}_{i-1}C(\theta_i - \underline{\theta}_i). \end{aligned} \tag{2.65}$$

Note that $\bar{\ell}_{i-1} \cdot \bar{\ell}_{i-1} = 1$ and $\bar{\ell}_i \cdot \bar{\ell}_{i-1} = C(\theta_i - \underline{\theta}_i)$ are used in deriving Eq. (2.65). As shown in Fig. 2.6, the active unit normal vector $\bar{n}_i$ can be obtained by rotating $-\bar{\ell}_{i-1}$ about $\bar{m}_i$ through an angle θ_i (see Eq. (1.25)). This leads to

$$\begin{aligned} \bar{n}_i &= \begin{bmatrix} n_{ix} & n_{iy} & n_{iz} & 0 \end{bmatrix}^T = \mathrm{rot}(\bar{m}_i, \theta_i)(-\bar{\ell}_{i-1}) \\ &= \begin{bmatrix} m_{ix}^2(1 - C\theta_i) + C\theta_i & m_{iy}m_{ix}(1 - C\theta_i) - m_{iz}S\theta_i & m_{iz}m_{ix}(1 - C\theta_i) + m_{iy}S\theta_i & 0 \\ m_{ix}m_{iy}(1 - C\theta_i) + m_{iz}S\theta_i & m_{iy}^2(1 - C\theta_i) + C\theta_i & m_{iz}m_{iy}(1 - C\theta_i) - m_{ix}S\theta_i & 0 \\ m_{ix}m_{iz}(1 - C\theta_i) - m_{iy}S\theta_i & m_{iy}m_{iz}(1 - C\theta_i) + m_{ix}S\theta_i & m_{iz}^2(1 - C\theta_i) + C\theta_i & 0 \\ 0 & 0 & 0 & 1 \end{bmatrix} \\ &\quad \begin{bmatrix} -\ell_{i-1x} \\ -\ell_{i-1y} \\ -\ell_{i-1z} \\ 0 \end{bmatrix}. \end{aligned} \tag{2.66}$$

Utilizing Eq. (2.65), Eq. (2.66) can be simplified as

$$\bar{n}_i = \left[\frac{(C\theta_i C\underline{\theta}_i + S\theta_i S\underline{\theta}_i)S\theta_i}{S\theta_i C\underline{\theta}_i - C\theta_i S\underline{\theta}_i} - C\theta_i\right]\bar{\ell}_{i-1} - \left[\frac{S\theta_i}{S\theta_i C\underline{\theta}_i - C\theta_i S\underline{\theta}_i}\right]\bar{\ell}_i, \tag{2.67}$$

where $S\theta_i$, $C\theta_i$, $S\underline{\theta}_i$ and $C\underline{\theta}_i$ are given in Eqs. (2.60), (2.61), (2.62) and (2.63), respectively.

2.5.2 *Unit Normal Vector of Reflective Boundary Surface*

Referring to Fig. 2.5, to determine the active unit normal vector $\bar{n}_i$ at any incidence point $\bar{P}_i$ on a reflective surface $\bar{r}_i$, it is first necessary to calculate the common normal vector $\bar{m}_i$ of the unit directional vectors of the incoming and outgoing rays (i.e., $\bar{\ell}_{i-1}$ and $\bar{\ell}_i$). Given the assumption $\theta_i \neq 0$, $\bar{m}_i$ can be obtained as

$$\bar{m}_i = \begin{bmatrix} m_{ix} & m_{iy} & m_{iz} & 0 \end{bmatrix}^T = \frac{\bar{\ell}_i \times \bar{\ell}_{i-1}}{S(2\theta_i)}, \tag{2.68}$$

where the incidence angle θ_i is determined by

$$C(2\theta_i) = \left|\bar{\ell}_{i-1} \cdot \bar{\ell}_i\right|. \tag{2.69}$$

Note that Eq. (2.69) is also applicable for an incidence angle equal to zero.

To simplify the expression for the unit normal vector $\bar{n}_i$, it is useful to have the following equation, obtained by taking the post cross product of Eq. (2.68) by $S(2\theta_i)\bar{\ell}_{i-1}$, i.e.,

$$\begin{aligned} S(2\theta_i)\left(\bar{m}_i \times \bar{\ell}_{i-1}\right) &= (\bar{\ell}_i \times \bar{\ell}_{i-1}) \times \bar{\ell}_{i-1} \\ &= \bar{\ell}_{i-1}(\bar{\ell}_i \cdot \bar{\ell}_{i-1}) - \bar{\ell}_i(\bar{\ell}_{i-1} \cdot \bar{\ell}_{i-1}) = -C(2\theta_i)\bar{\ell}_{i-1} - \bar{\ell}_i. \end{aligned} \tag{2.70}$$

Note that $\bar{\ell}_{i-1} \cdot \bar{\ell}_{i-1} = 1$ and $\bar{\ell}_i \cdot \bar{\ell}_{i-1} = -C(2\theta_i)$ are used in deriving Eq. (2.70). As shown in Fig. 2.5, the active unit normal vector $\bar{n}_i$ can be determined by rotating $-\bar{\ell}_{i-1}$ about $\bar{m}_i$ through an angle θ_i (i.e., Eq. (2.66)). Simplifying Eq. (2.66) using Eq. (2.70), the following expression is obtained for the unit normal vector $\bar{n}_i$ at any incidence point on the reflective surface when $\bar{\ell}_{i-1}$ and $\bar{\ell}_i$ are given:

$$\bar{n}_i = \frac{1}{2C\theta_i}\left(\bar{\ell}_i - \bar{\ell}_{i-1}\right) = \frac{1}{\sqrt{2\left(1 - \bar{\ell}_{i-1} \cdot \bar{\ell}_i\right)}}\left(\bar{\ell}_i - \bar{\ell}_{i-1}\right). \tag{2.71}$$

The fabrication of aspherical surfaces requires the use of high-precision manufacturing techniques in order to achieve the necessary surface accuracy and smoothness. Large aspherical lenses are typically produced using grinding and polishing techniques. Single-point diamond turning [35] is an emerging technique for fabricating large aspherical surfaces, and typically results in a better metallurgical structure than that produced by polishing and lapping. However, in using such a method, precise tool angle settings must be determined in advance in order to obtain the desired surface profile [40, 41]. The setting angles are determined by both the tool geometry and the normal vectors of the aspherical surface. Thus, as described above, Eqs. (2.67) and (2.71) are important not only in predicting the optical performance of the surface, but also in formulating the numerical codes required to machine the surface during the fabrication process.

References

1. Cornbleet S (1983) Geometrical optics reviewed: a new light on an old subject. Proc IEEE 71:471–502
2. Hamilton WR (1830) Supplement to an essay on the theory of systems of rays. Trans R Irish Acad 16:1–61
3. Silverstein L (1918), Simplified method of tracing rays through any optical system of lenses, prism and mirrors. Longmans, Green and Company, New York
4. Spencer CH, Murty MVRK (1962) General ray-tracing Procedure. J Opt Soc Am 52:672–678
5. Stavroudis ON (1951) Ray-tracing formulas for uniaxial crystals. J Opt Soc Am 52:187–191
6. Conrady AE (1929) Applied optics and optical design. Oxford University Press, New York, first edition, Part I, p. 413
7. Luneburg R (1965) Mathematical theory of optics, 3rd edn. Pergamon, New York, p 373
8. Born M, Wolf E (1980) Principles of optics, Chap. 14, 6th edn. Pergamon Press, p 668
9. Malacara D, Malacara Z (2004) Handbook of optical design, Section 3.5, Equation (3.37), 2nd edn. Marcel Dekker Inc. New York
10. Allen WA, Snyder JR (1952) Ray tracing through uncentered and aspherical surfaces. J Opt Soc Am A 42:243–249
11. Ford PW (1960) New ray tracing scheme. J Opt Soc Am 50:528–533
12. Pinto G (1979) A program for ray tracing through tilted and decentered optical surfaces. Opt Acta 65:1321
13. Hanssen JS (1982) Ray-tracing programs for spherical and aspherical surfaces. Appl Opt 21:2184
14. Kasper E (1984) On the numerical determination of optical focusing properties and aberrations. Optik 69:117–125
15. Montagnino L (1968) Ray tracing in inhomogeneous media. J Opt Soc Am 58:1667–1668
16. Buchdahl HA (1973) Rays in gradient index media: separable systems. J Opt Soc Am 63:46
17. Moore DT (1975) Ray tracing in gradient-index media. J Opt Soc Am 65:451–455
18. Moore DT (1980) Gradient-index optics. Appl Opt 19:1035–1038
19. Southwell WH (1982) Ray tracing in gradient-index media. J Opt Soc Am 72:908–911
20. Sharma A, Kumar DV, Ghatak AK (1986), Tracing rays through graded-index media. Appl Opt 21:984–987; 24:4367–4370 (1985); 25:3409–3412
21. Simon MC, Echarri RM (1983) Ray tracing formulas for monoaxial optical components. Appl Opt 22:354–360
22. Simon MC, Echarri RM (1986) Ray tracing formulas for monoaxial optical components: vectorial formulation. Appl Opt 25:1935–1939
23. Simon MC (1987) Refraction in biaxial crystals: a formula for the indices. J Opt Soc Am A 4:2201–2204
24. Yariv A, Yeh P (1984) Optical waves in crystals. Wiley, New York
25. Liang QT (1990) Simple ray-tracing formulas for uniaxial optical crystals. Appl Opt 29:1008–1010
26. Liang QT, Zheng XD (1991) Ray-tracing calculations for uniaxial optical components with curves surfaces. Appl Opt 30:31
27. Trollinger JD, Chipman RA, Wilson DK (1991) Polarization ray tracing in birefringent media. Opt Eng 30:461–466
28. Beyerle G, McDermid IS (1998) Ray-tracing formulas for refraction and internal reflection in uniaxial crystals. Appl Opt 37:7947–7953
29. Zhang WQ (1991) General ray-tracing formulas for crystal. Appl Opt 31:7328–7331
30. Nishidate Y, Nagata T, Morita S, Yamagata Y (2011) Raytracing method for isotropic inhomogeneous refractive-index media from arbitrary discrete input. Appl Opt 50:5192–5199
31. Feder D (1968) Differentiation of ray-tracing equations with respect to construction parameters of rotationally symmetric optics. J Opt Soc Am 58(11):1494–1505

32. Stavroudis O (1976) Simpler derivation of the formulas for generalized ray tracing. J Opt Soc Am 66(12):1330–1333
33. Lu CH, Sung CK (2013) Skew ray tracing and sensitivity analysis of hyperboloid optical boundary surfaces. Optik—Int J Light Electron Optics 124:1159–1169
34. Smith WJ (2001) Modern optical engineering, 3rd edn. Edmund Industrial Optics, Barrington, N.J
35. Haisma J, Hugues E, Babolat C (1979) Realization of a bi-aspherical objective lens for the philips video play system. Opt Lett 4:70–72
36. Lin PD, Tsai CY (2012) Determination of first-order derivatives of skew-ray at aspherical surface. J Opt Soc Am A 29:1141–1153
37. Gutiérrez CE (2013) Aspherical lens design. J Opt Soc Am A 30:1719–1726
38. Lin PD, Tsai CY (2012) Determination of unit normal vectors of aspherical surfaces given unit directional vectors of incoming and outgoing rays. J Opt Soc Am A 29:174–178
39. Lin PD, Tsai CY (2012) Determination of unit normal vectors of aspherical surfaces given unit directional vectors of incoming and outgoing rays: reply. J Opt Soc Am A 29:1358
40. Boothroyd G (1975), Fundamentals of metal machining and machine tools, Chap. 7. McGraw-Hill, New York, NJ
41. Biddut AQ, Rahman M, Neo KS, Rezaur KM, Sawa M, Maeda Y (2007) Performance of single crystal diamond tools with different rake angles during micro-grooving on electroless nickel plated die materials. Int J Adv Manuf Technol 33:891–899

http://www.springer.com/978-981-10-2298-2

Advanced Geometrical Optics
Lin, P.D.
2017, XXIV, 460 p. 222 illus., 193 illus. in color.,
Hardcover
ISBN: 978-981-10-2298-2